

MASTER

A LOW-PRESSURE APPROACH
TO
THE FORMATION AND STUDY
OF
EXCIPLEX SYSTEMS

Final Report
Contract No. EY-76-S-02-2810, 003

Dr. George Sanzone
Department of Chemistry
Virginia Polytechnic Institute and State University
Blacksburg, Virginia 24061



June, 1981

Approved for public release
by the Defense Technical Information Service
Distribution Statement A

ABSTRACT

Under this contract, the following goals were set.

1. Development and construction of an experimental system for the study of the kinetics of excimers, and demonstrate the validity of the low-pressure approach to such studies. The apparatus was to consist of the following:
 - a) Cluster-molecular-beam source of van der Waals dimers and higher oligomers;
 - b) Modulated-beam mass spectrometer;
 - c) Low-energy electron beam for the production of excimers;
 - d) Vacuum-ultraviolet to visible detection and photon-counting system to monitor excimer emission;
 - e) Flash-excited tunable laser for studies of resonant self-absorptions.
2. Form Ar_2 in its van der Waals ground state.
3. Produce Ar_2^* by electron bombardment of Ar_2 .
4. Perform fluorescence and photon absorption studies of Ar_2^* .

At the end of the contract period, goals 1 and 2 have been met; experiments 3 and 4 have been designed.

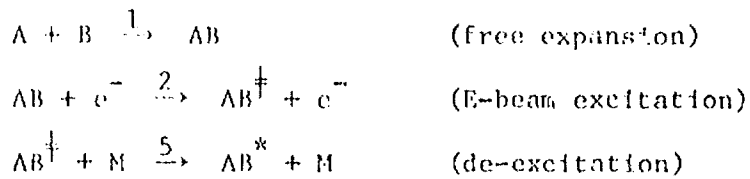
CONTENTS

I: INTRODUCTION	1
II: THE LOW-PRESSURE APPROACH	3
II.A: The Underexpanded Free Jet	6
II.B: Dimer and Oligomer Formation	11
II.C: Design of the Dimer Beam	13
II.D: Calibration Experiments	20
II.E: Calculated Dimer Concentrations	25
III: THE STATUS OF THE APPARATUS	31
III.A: Mass Spectrometers	34
III.B: Excitation Electron Gun	38
III.C: Photon Detection	41
IV: FORMATION OF EXCIMERS	43
IV.A: Visible to Vacuum Ultraviolet Spectra	44
IV.B: Electron Excitation Cross Sections	44
IV.C: Reactive Cross Sections	44
IV.D: Lifetimes	45
IV.E: Resonant Self-Absorption	45
IV.F: Upward-Bound Transitions	46
IV.G: Photoionization of Excited States	47
V: MERCURY AND MERCURY-INERT GAS DIMERS	49
VI: CALCULATED POTENTIAL ENERGY CURVES	50
VII: REFERENCES	51
VIII: PERSONNEL	56

I: INTRODUCTION

Among the potential lasing materials for laser-fusion research are the rare gas excimers and other bound-unbound emitters.^[1] Although considerable information on these materials is becoming available, the absence of fundamental data prevents us from applying this information to new systems. In our work, we have developed a promising new technique for basic research on both known and new excimer systems. In addition, the apparatus built to demonstrate our technique is capable of application to a number of fundamental problems beyond the field of laser fusion.

A system was designed and built in which excimers can be formed from their van der Waals ground states. Low temperatures (typically 5K) obtained in a free-jet expansion have been used to produce high, steady-state concentrations of van der Waals dimers and other oligomers. These, in turn, can be excited by low-energy, resonant electron bombardment to yield excimers and exciplexes. The mechanism, illustrated in Figure 1, is as follows:



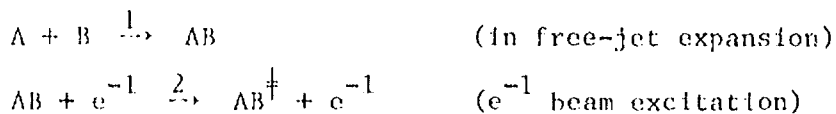
The excited states of the dimers, oxides, and halides of inert gases are candidates for study.^[2] For any laser system, it is necessary to study both primary and secondary photo-processes;^[3] we can do both. With our technique, we can probe the relative rates of electron pumping of excited-state manifolds and, ultimately, the preferentially pumped

vibronic states within each manifold; we can also consider reactive quenching of emission, as well as collision- and noncollision-induced intersystem crossing. Collision-induced crossing is especially interesting to us; it is important not only for systems like the inert-gas oxides, but also for applications of RRKM theory to systems which exhibit such crossing, e.g. N_2O .^[4]

Although the work originally focussed only on the kinetics of excimer formation and on reactive and radiative lifetimes, the scope of our project was expanded to include another source of excimer depletion: near-resonant self absorption of 1sing emission. If this process is efficient, especially at high pressures, it could lead to a serious loss of photons via the production of more highly excited (perhaps Rydberg) states. The experimental system can also be used to measure appearance potentials of van der Waals molecules and photionization cross sections of excimers.

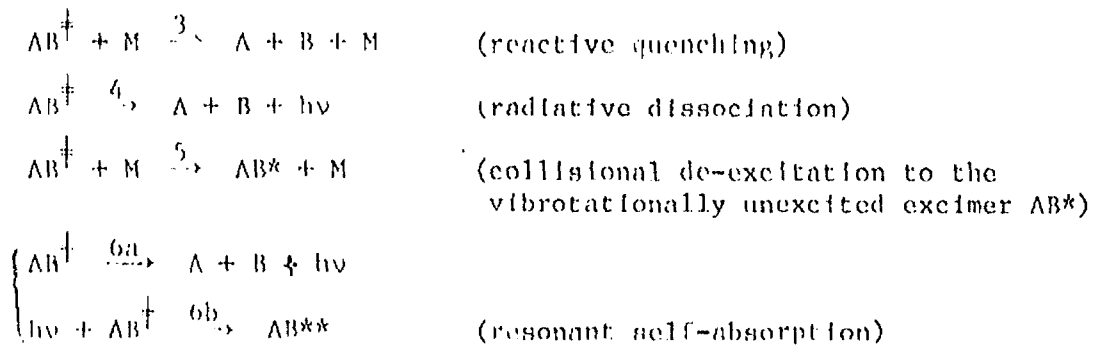
II: THE LOW-PRESSURE APPROACH

At the high pressures generally employed, fundamental processes in lasing materials are difficult to study; rapid collisional quenching complicates the study of excitation, de-excitation, and radiative kinetics. Consequently, instead of using high pressures, we have elected to use the low temperatures obtained in a free-jet expansion for the production of high, steady-state concentrations of van der Waals dimers and oligomers. These molecules are then excited by low-energy, resonant electron bombardment to produce excimers or exciplexes, probably in vibrotionally excited states. The formation mechanism is



In these reactions, A might be an inert-gas atom while B could be another inert-gas atom, an oxygen atom, or a halogen atom. The procedure is based on the fact that dimers and oligomers form in the first steps of condensation in a jet expansion;^[5] it assumes that excitation by electron bombardment is a Franck-Condon process.

Once formed, an excimer can suffer a number of fates, as represented by the following paths for excimer depletion:



In addition, the vibrotationally unexcited AB^* can itself undergo reactive quenching, radiative dissociation, and resonant self-absorption. The total mechanism (embodied in the above equations) is shown schematically in Figure 1.

The use of resonant, low-energy electron pumping is not restricted to species produced in a jet expansion. Consequently, our experimental system could also be used to study excited states of stable species, for example CO^* , CO_2^* and CS^* .

The experiments proposed were difficult, but worth the attempt. Indeed, if it were not for a bizarre set of problems with personnel (See section VIII), even more data would have been obtained. As it is, experiments continue, even though this contract has expired.

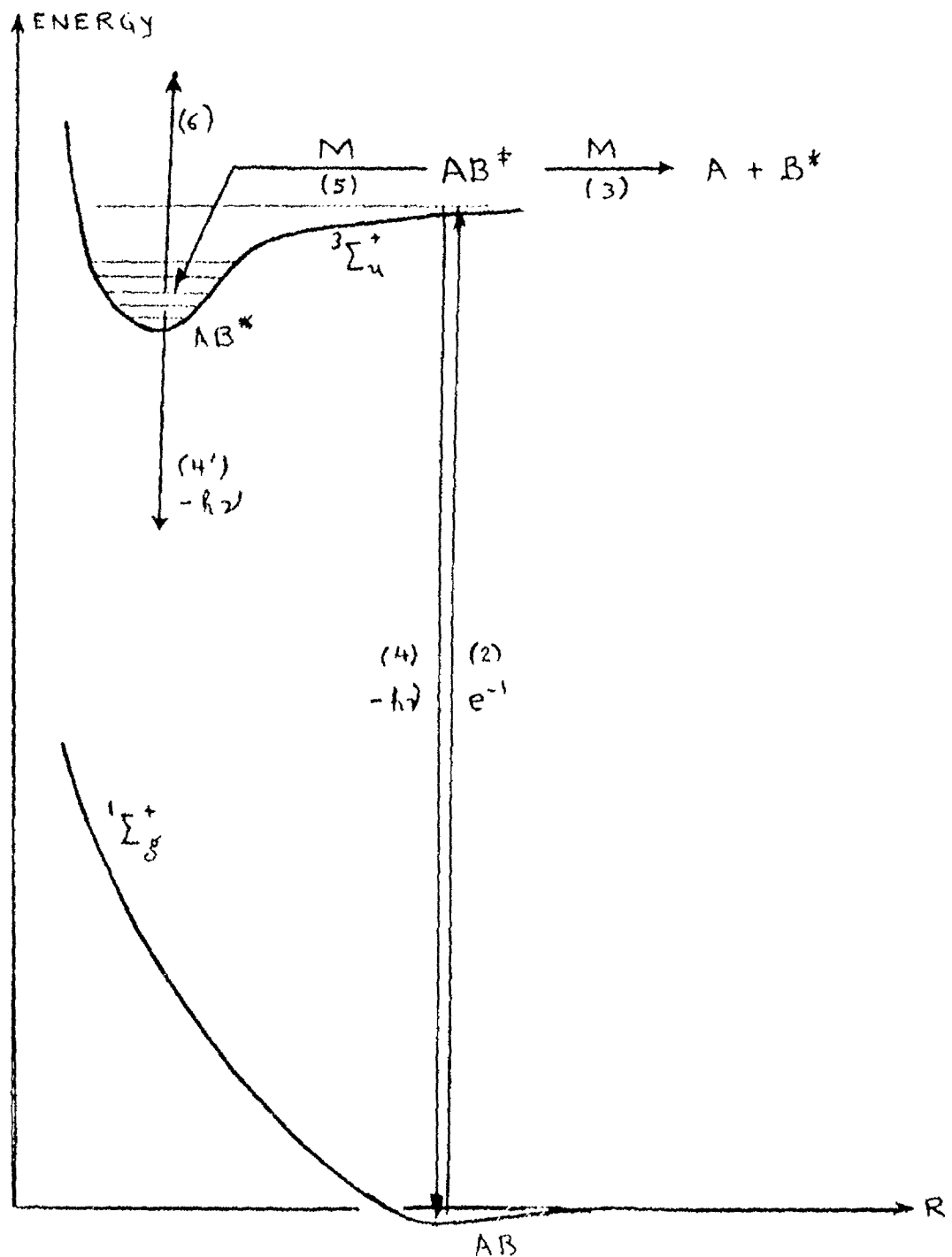


FIGURE 1. FORMATION MECHANISM FOR AB^* .
 VAN DER WAALS COMPLEX AB IS
 PRODUCED IN A FREE-JET EXPANSION.

II.A: THE UNDEREXPANDED FREE JET

A transition from subsonic to supersonic flow can occur without shock waves in a nozzle which has a throat.^[6] For sufficiently great pressure ratios across a nozzle, the flow at the throat goes transonic; when this occurs, the pressures downstream from the throat become independent of the ambient, expansion-chamber pressure, p_a . If the nozzle exit pressure, p_e , is equal to p_a , then the nozzle flow is said to be ideal, otherwise it is non-ideal.

Two classes of non-ideal, supersonic nozzle flow can be distinguished, depending upon whether $p_a < p_e$; their significance for jet formation has been reviewed.^[7] If $p_a > p_e$, a shock pattern forms in the nozzle. The lower the ambient pressure, the further downstream from the throat will be the position of this shock. For sufficiently low p_a , the shock pattern is positioned at the nozzle exit. If p_a is further lowered, but is greater than p_e , the adjustment of the flowing gas to the exit chamber pressure takes place external to the nozzle. The shock pattern takes the form of a plume which has its base at the nozzle exit and is terminated by another shock called the Mach disk. (See Figure 2.)

If $p_a < p_e$, the adjustment to ambient pressure must again take place external to the nozzle, i.e. in the free jet. This class, the underexpanded jet, is important for this research. Maximum mass flow, \dot{m}_{max} , obtains when the flow is isentropic with a sonic velocity at the throat:^[7]

$$\dot{m}_{max} = \left\{ \frac{2}{\gamma+1} \right\}^{\frac{\gamma+1}{2(\gamma-1)}} \cdot p_0 \cdot \left(\frac{\gamma R T_0}{2 \pi} \right)^{1/2}$$

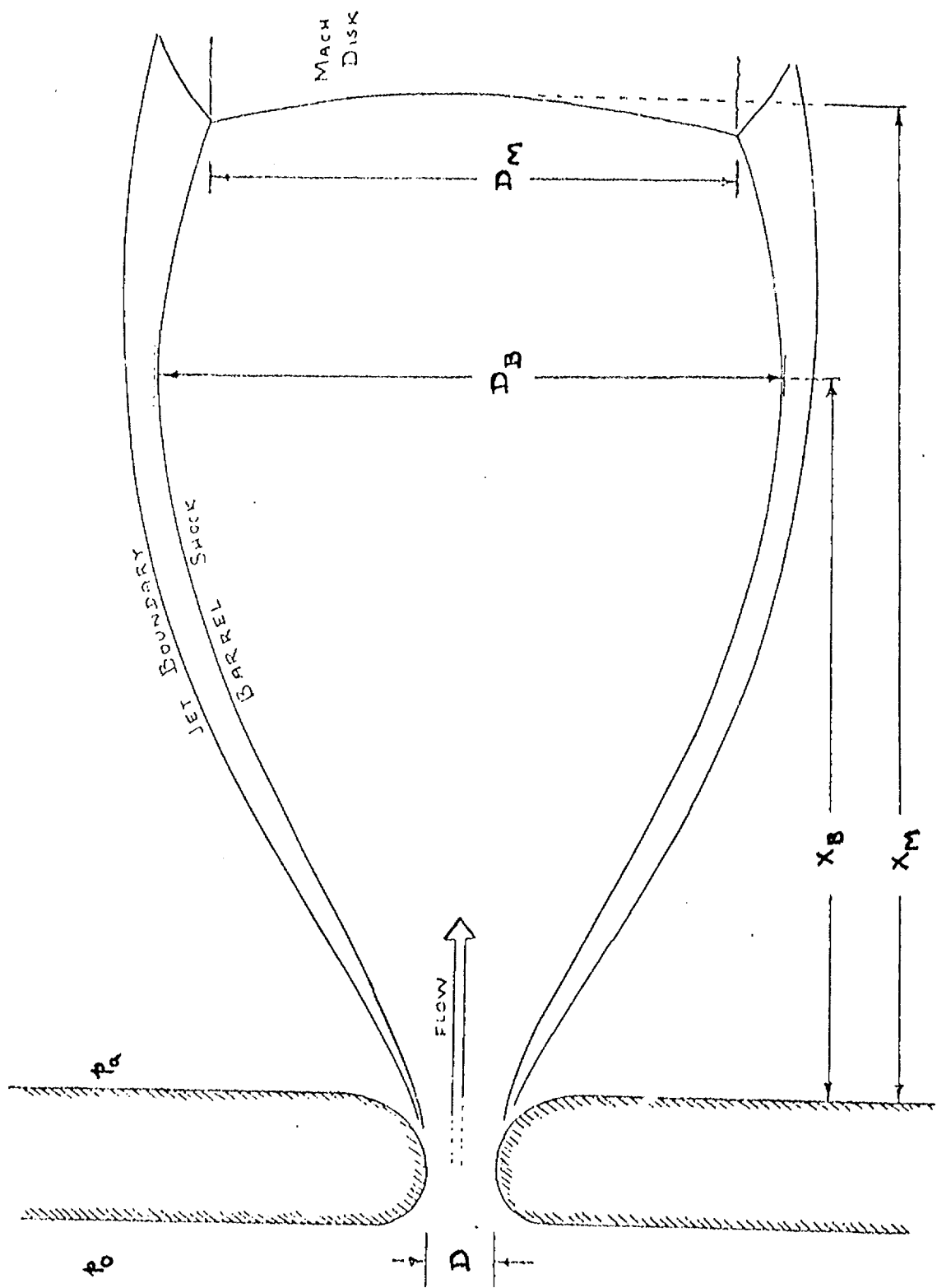


Figure 2.

The Underexpanded Free Jet

In this equation, p_o , T_o , and γ are the density, temperature, and heat capacity ratio in the stagnation state (reservoir conditions); M is the molecular weight of the gas, and A is the nozzle area (at the throat). The structure of the underexpanded free jet has been the subject of considerable study.^[7,8] The shape of this jet has been well characterized by Bier and Schmidt,^[9] Crist,^[10] and others. All principal radii and diameters which characterize the jet geometry have been found to scale linearly with nozzle diameter, D . For nozzle pressure ratios, (p_o/p_a) , from 10 to 300,000 (where p_o is the stagnation pressure) and for stagnation temperatures to 4200 K,

$$x_m = 0.67 D (p_o/p_a)^{1/2}.$$

(See Figure 2.) Streamlines in the jet radiate from a virtual point source located a distance x_s downstream from the nozzle exit.^[11] This distance correlates with the number, f , of active degrees of freedom in the gas.^[7]

$$x_s = D [0.20 f - 0.56]$$

For $x > 4D$, the flow Mach number along the jet centerline can be estimated:

$$M \approx \frac{5.43}{\gamma} \left\{ \frac{x-x_s}{D} \right\}^{\gamma-1}.$$

Interest in the use of nozzle expansions as high-intensity sources of molecular beams began with the work of Kantrowitz and Gray.^[12,13] They predicted an intensity gain (over oven beams) by a factor of $(1/2)\gamma M^2$; the Mach number is calculated at the position of a skimmer. (The objective is to sample only the jet core). The predicted gain has never been fully realized; deviations from this limit increase with p_o . Originally, it was believed that observed deviations were due to dimerization^[14]; a more likely cause is scattering of the beam by background molecules.^[15]

Measurement of the velocity distribution in free jets revealed the existence of a maximum or terminal flow Mach number, M_t .^[16] Anderson and Fenn later showed this limit depends upon the nozzle Knudsen number, K , as follows^[17]:

$$M_t = 1.17 K^{-0.4}.$$

This relation gives the condition for which the collision rate in the gas becomes too low to sustain the continuum expansion; the velocity distribution and translational temperature "freezes".

To the extent that the free-jet expansion approximates a point-source flow, the expansion problem has been solved theoretically.^[18-20] The stress tensor is assumed to have anisotropic pressure components: p_{11} in the direction of the jet axis, and p_{\perp} in the direction transverse to this axis. This, in turn, introduces two translational temperatures, T_{11} and T_{\perp} , which are only equal at eqi librium. It is found that T_{11} gradually freezes in a spherical, point-source expansion, but T_{\perp} does not freeze. The terminal Mach number for a hard-sphere (monatomic) gas is predicted to be proportional to $K^{-0.40}$. The freezing of T_{11} and the non-freezing of T_{\perp} have been experimentally confirmed.^[21-23] For spherical expansions of polyatomic gases, the internal temperature freezes rapidly while both T_{11} and T_{\perp} are still decreasing; further along in the expansion, T_{11} freezes, but T_{\perp} never freezes.^[24]

Although the axial temperature freezes, the density in the jet monotonically decreases as a function of distance x from the nozzle exit. If x is much greater than the nozzle diameter D , then the density in the jet is well approximated by

$$\rho = 0.018 \left\{ \frac{Y^2}{Y-1} \right\}^{\frac{1}{Y-1}} \left\{ \frac{D}{x} \right\}^2 \rho_0 ;$$

here, ρ_0 is the reservoir or stagnation density.

One additional property of the underexpanded free jet is its start-up time, t . A lower limit for this quantity may be estimated: [25]

$$t = \frac{0.0304}{c_0} \frac{x_B D}{D_B} \left\{ \frac{5.43}{Y} \right\}^{5/2} \left\{ \frac{x}{D} \right\}^{\frac{5(Y-1)}{2}}.$$

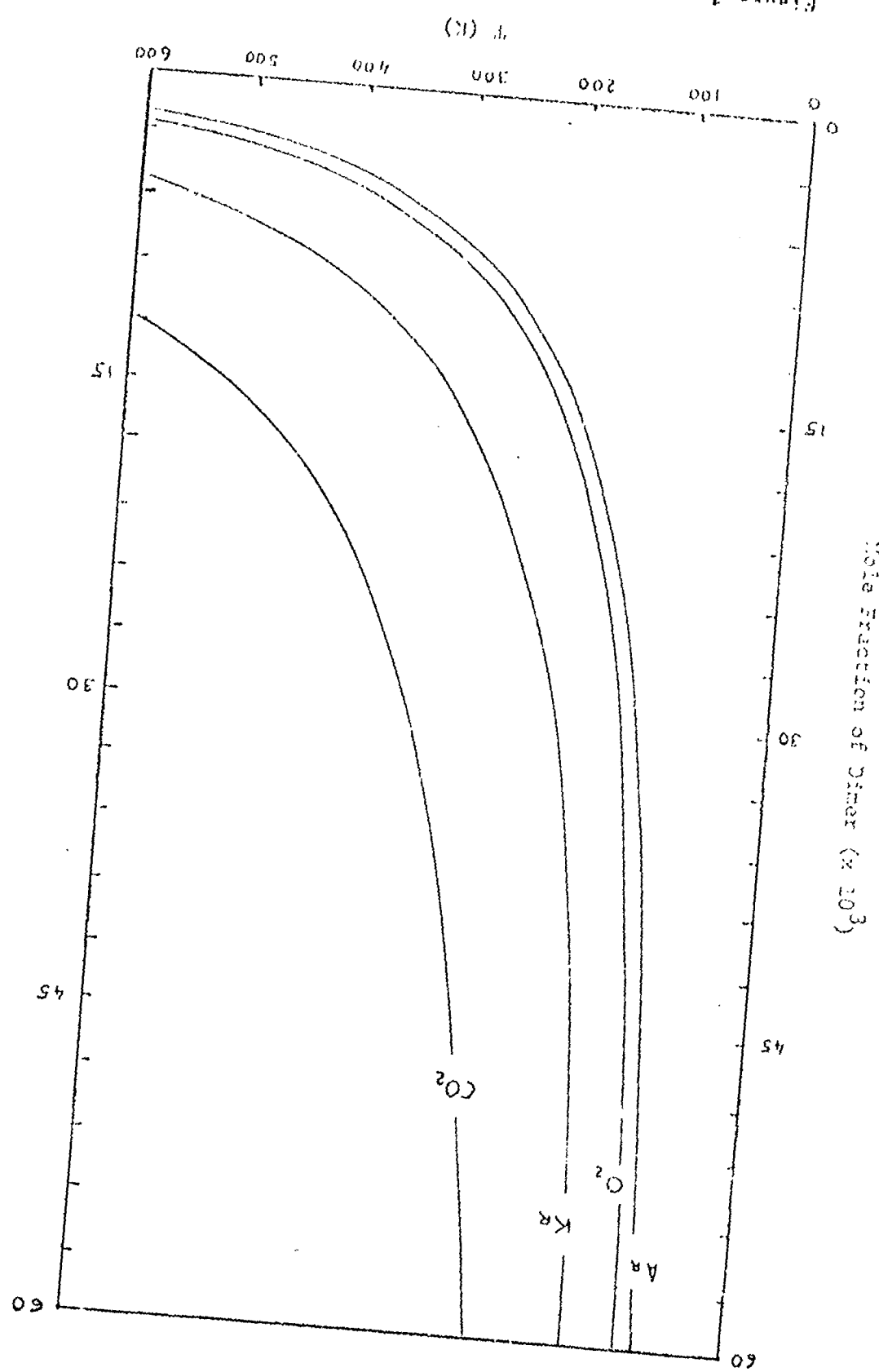
In this expression, x_B is the distance from the nozzle throat to the position of the greatest diameter of the barrel shock, D_B , (Figure 2); c_0 is the stagnation-state sound speed. Values of D_B/x_B are available for a number of gases. [19,20]

II.B: DIMER AND OLIGOMER FORMATION

Gases which were originally highly unsaturated can become highly supersaturated in a free-jet expansion. Although supersaturation can be reached in the subsonic portion of a nozzle expansion, condensation actually begins in the supersonic region.^[26] Condensation proceeds by way of the formation of dimers and higher clusters in homogeneous nucleation reactions; these condensation nuclei are carried along in the flow. Milne and Greene found that Argon clusters up to Ar₁₀ lagged the argon jet velocity by no more than 10 percent.^[27] The theory of nozzle flow in which the gas and condensation nuclei move with the same speed has been reviewed.^[28]

Bier and Hagena reported that for different-sized nozzles, similar condensation occurs at about the same nozzle Knudsen number.^[29] This is consistent with the finding that dimer concentration is a function of both orifice diameter and stagnation pressure.^[30] At fixed source pressures, Milne and Greene found that the concentration of Ar₂ increased exponentially with orifice diameter^[31]; in their studies, concentrations of oligomers in N₂, O₂ and NO were found to be several orders of magnitude lower than that of the dimer Ar₂. In general, the molecular dimer concentrations will be expected to be lower than inert-gas dimer concentrations because of meta-stability.^[32] Tables of inert-gas-dimer^[33] and oligomer^[34] equilibrium concentrations are available. See Figure 3. Observed concentrations may, however, be dictated by kinetic rather than by equilibrium factors; for example, the dimer of water has been observed at levels as high as 50% of the parent molecule.^[35] Increased oligomer concentrations have also been produced with gas mixtures.^[36]

Figure 3. Note fraction of Dimer (341)



III.C: DESIGN OF THE DIMER BEAM

As indicated above, dimers and oligomers in our studies have been formed in a free-jet expansion. A major experimental task has been the development of the nozzle-source cluster beam. Design equations and criteria were obtained, both from the literature and original derivations; these are presented in Tables I and II. We soon recognized that jet geometry is virtually independent of the conditions in the stagnation chamber, but is determined principally by system pumping speeds.^[37] This led to the design of a pulsed beam system. Although this added the mechanical design of a pulsed nozzle to our problems, it also gave us an important new control parameter; variation of stagnation chamber conditions has been given a real function in the control of cluster size. An important side-result of pulsed operation is that stagnation pressures of two atmospheres can be used to give jet performance comparable to that normally obtained at 100 atmospheres.^[37]

In addition to variation of nozzle duty cycle, the concentration of a selected oligomer can be optimized through control of the following experimental parameters (see Figures 4):^[39]

- Skimmer-to-nozzle distance (L_o),
- Orifice diameter (D),
- Stagnation pressure (p_o),
- Stagnation temperature (T_o).

Although nozzle shape is an important factor in conventional nozzle-beam design, it is unimportant for dimer studies. A study of cluster intensity for various nozzle shapes revealed that reported intensity increases were due to the formation of beams with larger average cluster size; the

intensity of dimers, trimers and other lower-oligomers does not change with nozzle size. This led to the use of a sonic nozzle in our studies.

TABLE I: CLUSTER BEAM EQUATIONS

Property	Relation
1. Nozzle Knudsen No.	$K \equiv \frac{\lambda_0}{D}$
2. Skimmer Knudsen No.	$K_{\text{skimmer}} \equiv \frac{\lambda_+}{D_{\text{skimmer}}}$
3. Mach Disk Knudsen No.	$K_{MD} \equiv \frac{\lambda_+}{D_{MD}}$
4. Nozzle Maximum Mass Flow Rate	$\frac{dm}{dt} = \left\{ \frac{2}{\gamma+1} \right\}^{\frac{\gamma+1}{2\gamma-2}} \rho_0 \frac{\pi D^2}{4} \left\{ \frac{\gamma R T_0}{M} \right\}^{1/2}$
5. Centerline Jet Density	$\rho = \left\{ \frac{0.0678}{\gamma-1} \right\}^{\frac{1}{\gamma-1}} \left\{ \frac{D}{x} \right\}^2 \rho_0$
6. Location of Mach Disk	$x_{MD} = 0.67 D \left\{ \frac{\rho_0}{\rho_+} \right\}^{1/2}$
7. Location of Virtual Source Point	$x_p = D (0.20 f - 0.56)$
8. Mach Number of Flow	$Ma = \frac{5.43}{\gamma} \left\{ \frac{x-x_p}{D} \right\}^{\gamma-1}$
9. Terminal Mach No.	$Ma_T = 1.17 K^{-0.4}$
10. Location of Onset of Background Penetration	$x_+ = 0.6 \frac{D}{K}$
11. Jet Expansion Chamber Background Pressure	$p_+ = \frac{2.86 \rho_0 D^2}{S} \left\{ \frac{T_0}{M} \right\}^{1/2}$
12. Jet Start-up Time	$t_{\text{rise}} = \frac{0.0304}{c_0} \frac{x_{BS}}{D_{BS}} D \left\{ \frac{5.43}{\gamma} \right\}^{5/2} \left\{ \frac{x}{D} \right\}^{\frac{5(\gamma-1)}{2}}$

Property	Relation
13. Jet Decay-Time	$t_{fall} = \frac{x_{skimmer}}{c_{+}}$
14. Maximum Flow Angle Prandtl-Mayer expansion	$\phi = \frac{\pi}{2} \left(\frac{\gamma+1}{\gamma-1} \right)^{1/2} - \frac{\pi}{2}$

Symbols Used In Table I:

ρ = Density	D = Diameter	S = Pumping Speed
γ = Heat capacity ratio	m = Mass	T = Kelvin Temperature
λ = Mean free path	M = Molar Mass	X = Distance From Nozzle Exit
c = Speed of Sound	p = pressure	f = Thermo degrees of Freedom

Subscripts:

- o denotes stagnation chamber
- $+$ denotes jet-chamber background
- BS denotes properties of jet barrel shock

TABLE II: DESIGN CRITERIA [37-39]

For jet formation:

$$K \leq 0.3$$

For negligible skimmer interference:

$$K_{\text{skimmer}} > 50 \quad \text{is OK.}$$

$$K_{\text{skimmer}} < 1 \quad \text{is OK.}$$

$$1 < K_{\text{skimmer}} < 50 \quad \text{is NoK.}$$

For negligible effect on jet properties:

$$x_{\text{skimmer}} \leq \frac{1}{2} x_{\text{MD}}$$

For similar cluster intensity and size distribution, two scaling laws have been suggested in the literature:

$$\left\{ p_0 D^{1/2} T_0^{-2.375} \right\} = \text{constant}$$

$$\left\{ p_0 D T_0^{-2.50} \right\} = \text{constant}$$

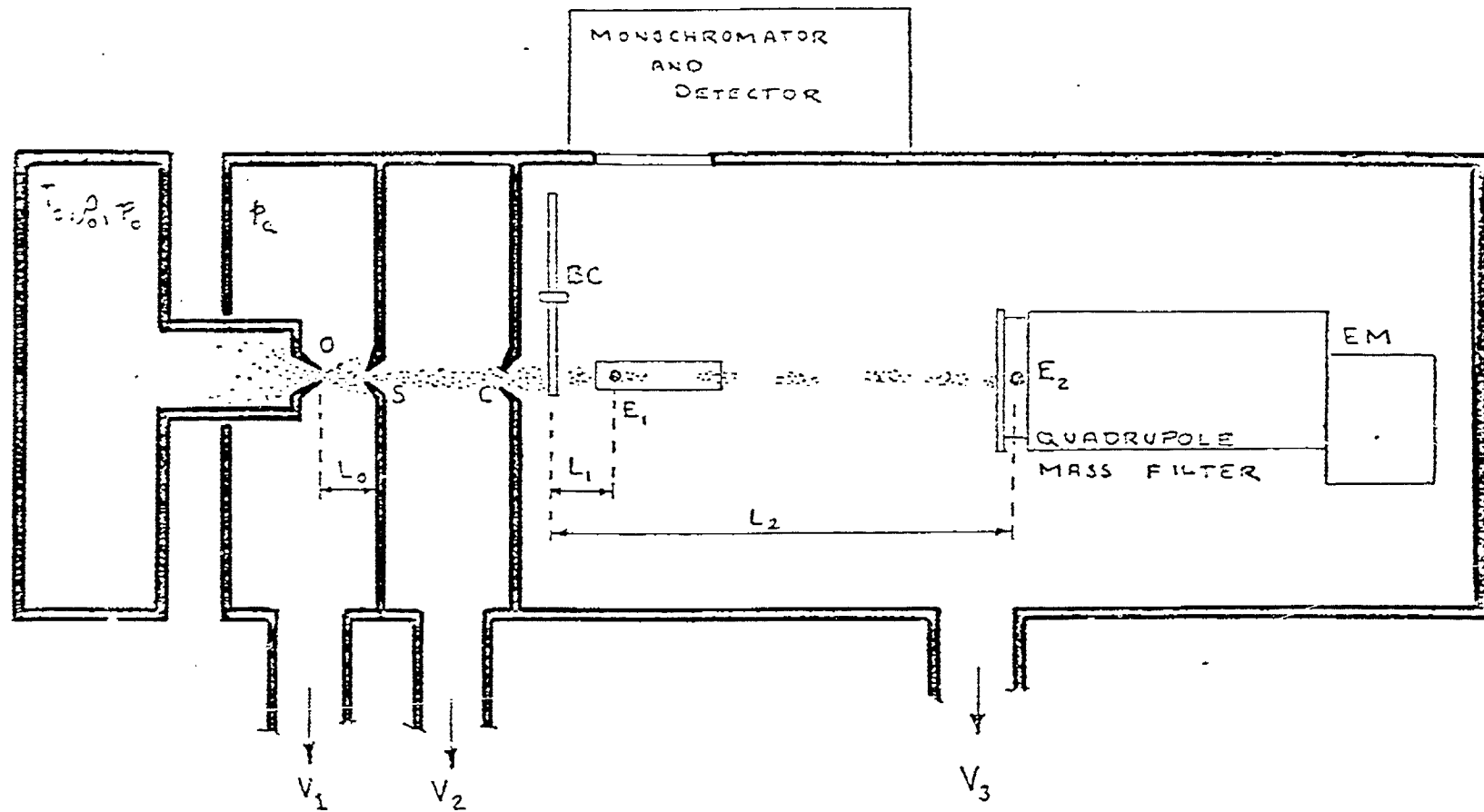


Figure 4 : Experimental Apparatus

Orifice O; Skimmer S; Collimator C; Vacuum Pumps V_1 , V_2 , V_3 ; Beam Chopper BC; Excitation Electron Beam E_1 ; Analytical Electron Beam E_2 ; Electron Multiplier EM. Distances L_0 , L_1 , L_2 are variable

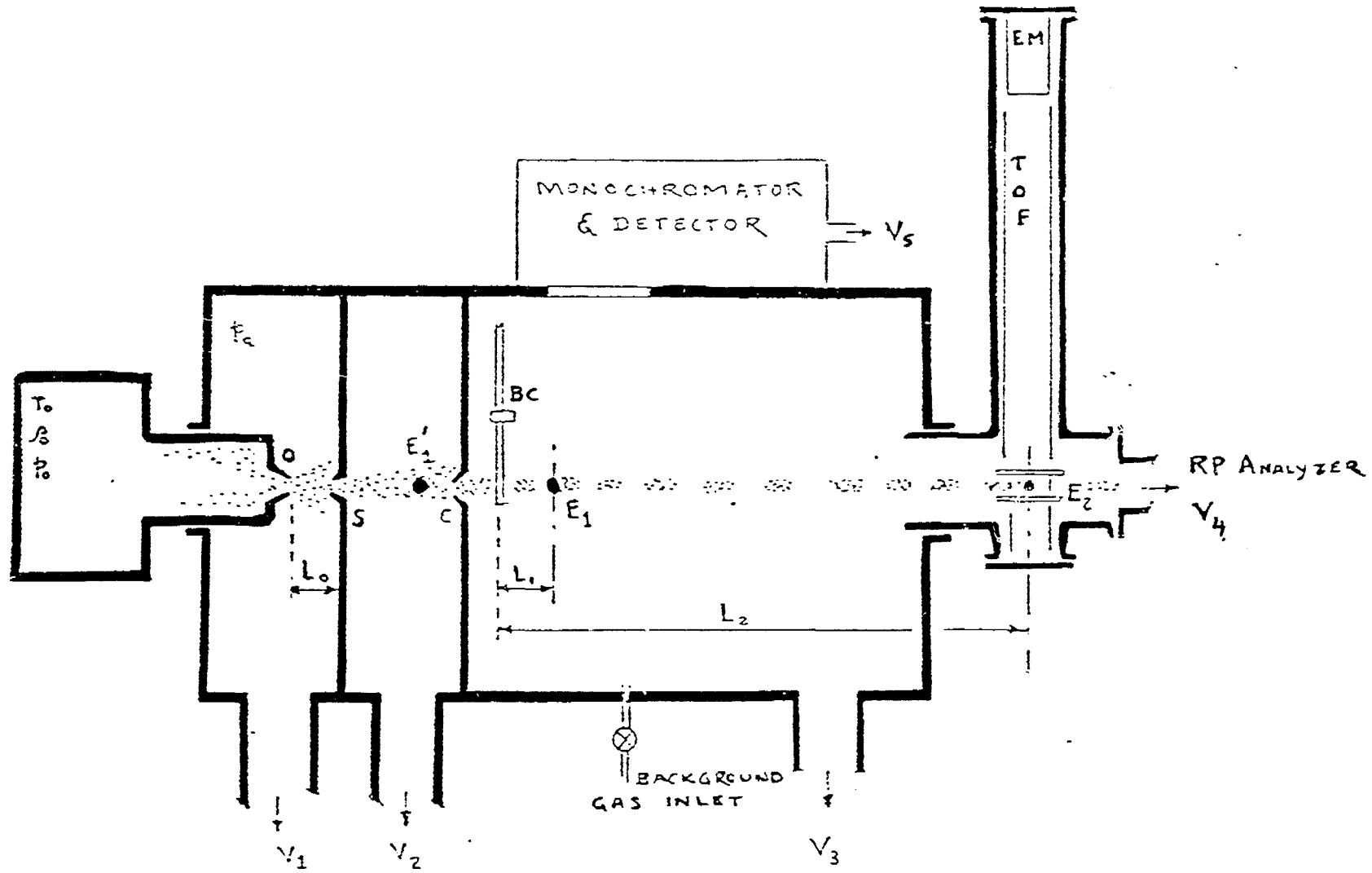
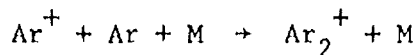


Figure 5: Experimental Apparatus

Orifice S; Skimmer S; Collimator C; Vacuum Pumps V_1 , V_2 , V_3 , V_4 , V_5 ; Beam Chopper BC; Excitation Electron Beam E_1 or E'_1 ; Analytical Electron Beam E_2 ; Electron Multiplier EM; Time-of-Flight Mass Analyzer TOF. Note: Distances L_0 , L_1 and L_2 are variable.

II.D: CALIBRATION EXPERIMENTS

Molecular beam composition has been monitored with modulated-beam mass spectrometry. The system includes a laboratory-built mechanical chopper, a lock-in amplifier, and either a time-of-flight (TOF) or quadrupole mass spectrometer. Once the pulsed nozzle source was incorporated, the mechanical chopper was removed; detection now is synchronized with nozzle opening. With pulsed dimer formation, we eliminate contributions to the Ar_2^+ signal from the background recombination process:



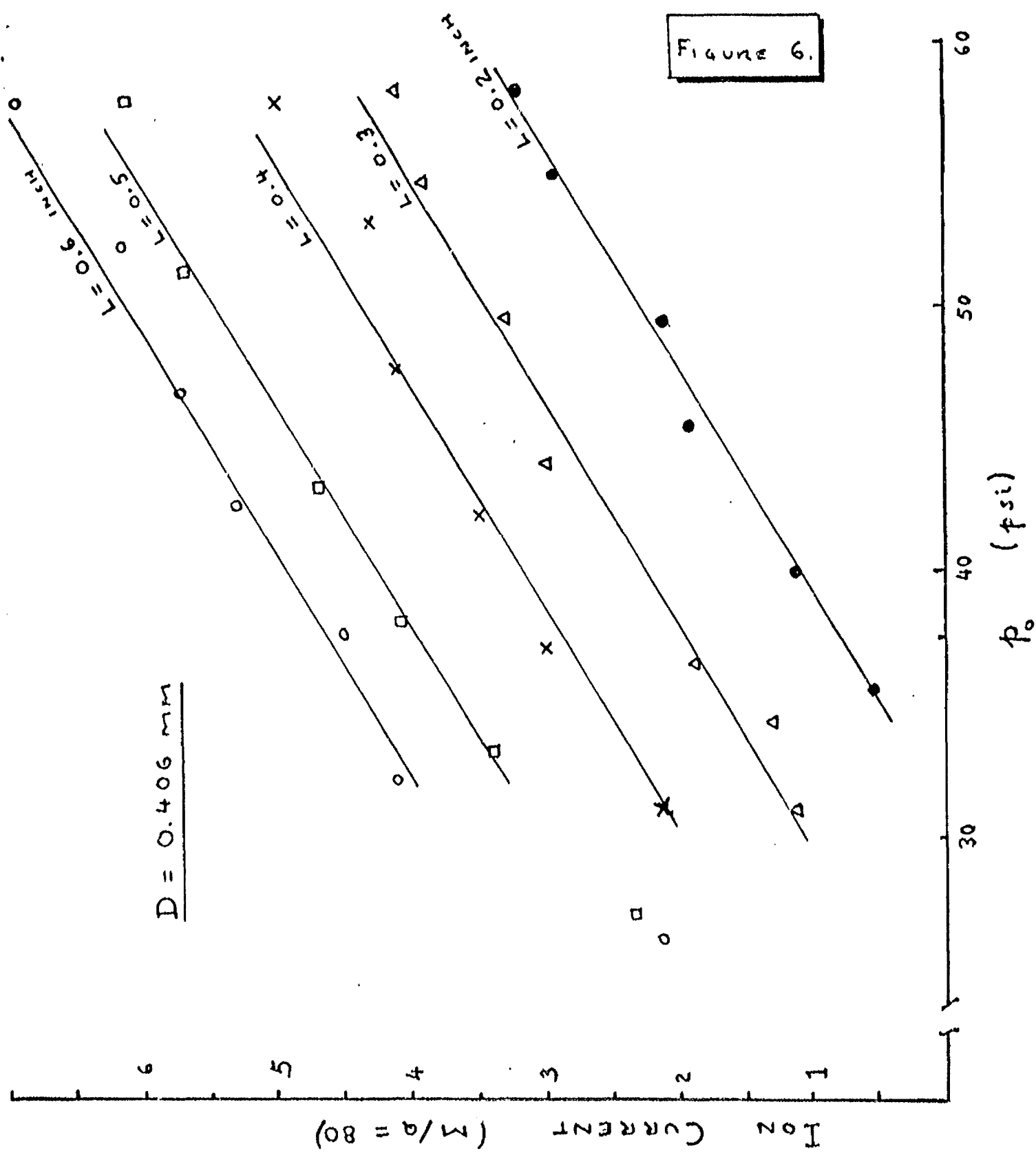
Single pulses of Ar_2^+ were first measured with a storage oscilloscope, and later with a Biomation transient recorder. Argon dimer was monitored as a function of the following experimental parameters: nozzle diameter, stagnation temperature, stagnation pressure, and nozzle-to-skimmer distance. Results are reported in Figures 6 through 9.

For nozzle diameters $D < 0.5$ mm, argon dimer formation obeyed one of the Laws of Corresponding Jets (See Table II).

$$p_o D T^{-5/2} = \text{constant.}$$

Probably because of inadequate pumping speed, data for $D \geq 0.5$ mm did not obey a Law of Corresponding Jets. It was also found that Ar_2 formation kinetics was third-order in argon stagnation pressure. Attainment of third-order kinetics had been selected as a key diagnostic of proper nozzle performance.

FIGURE 6.



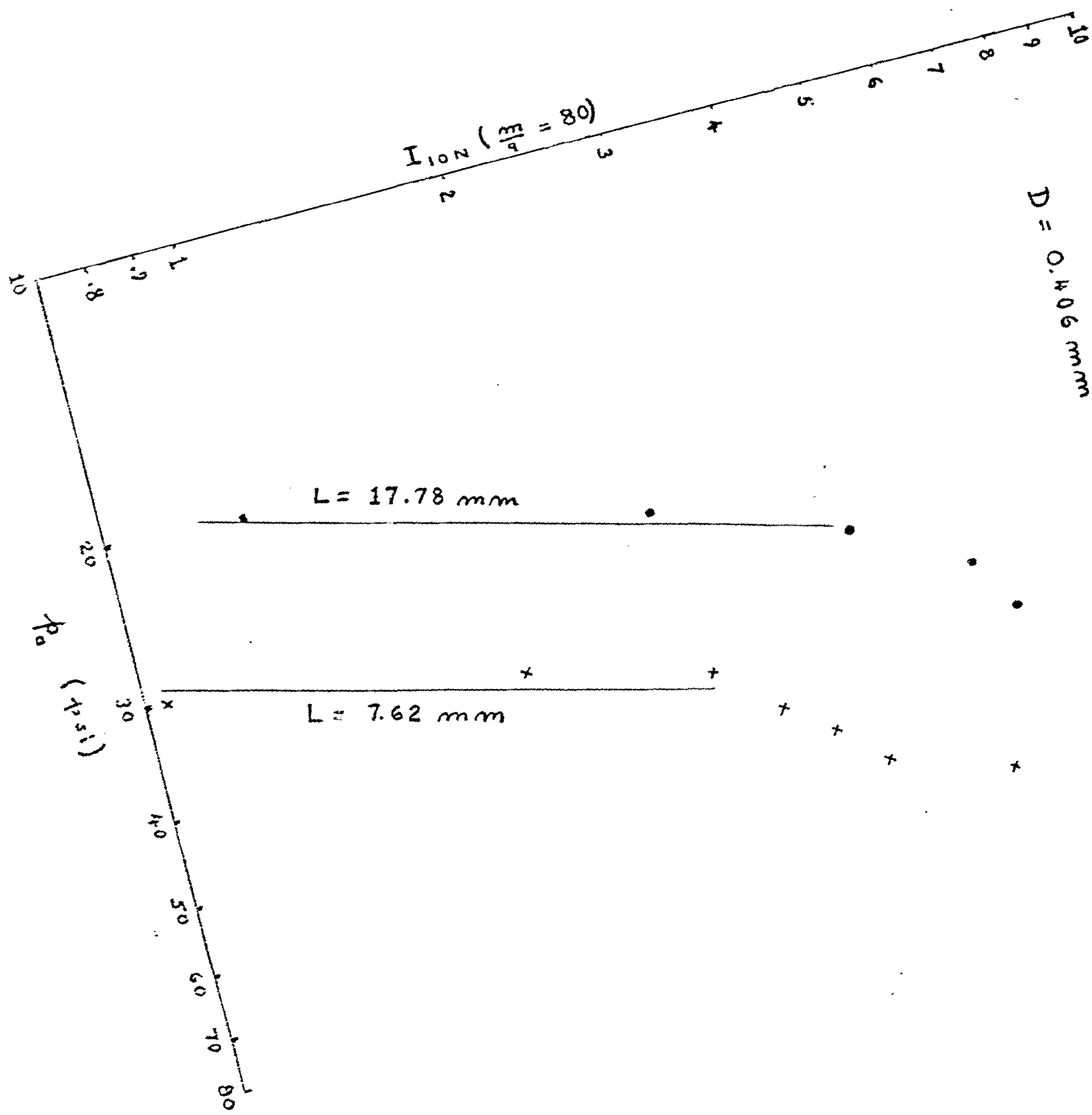


FIGURE 7

Figure 8

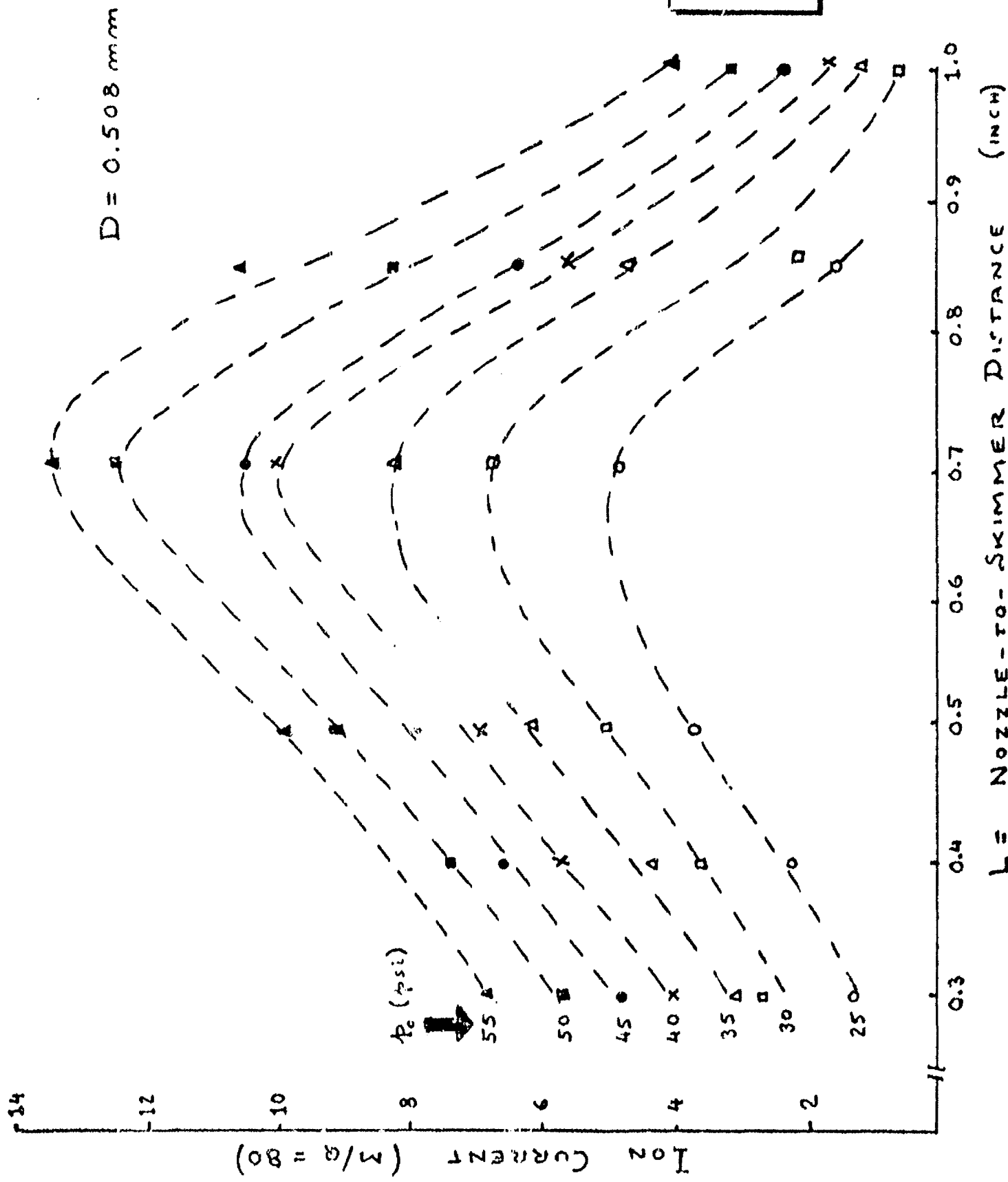
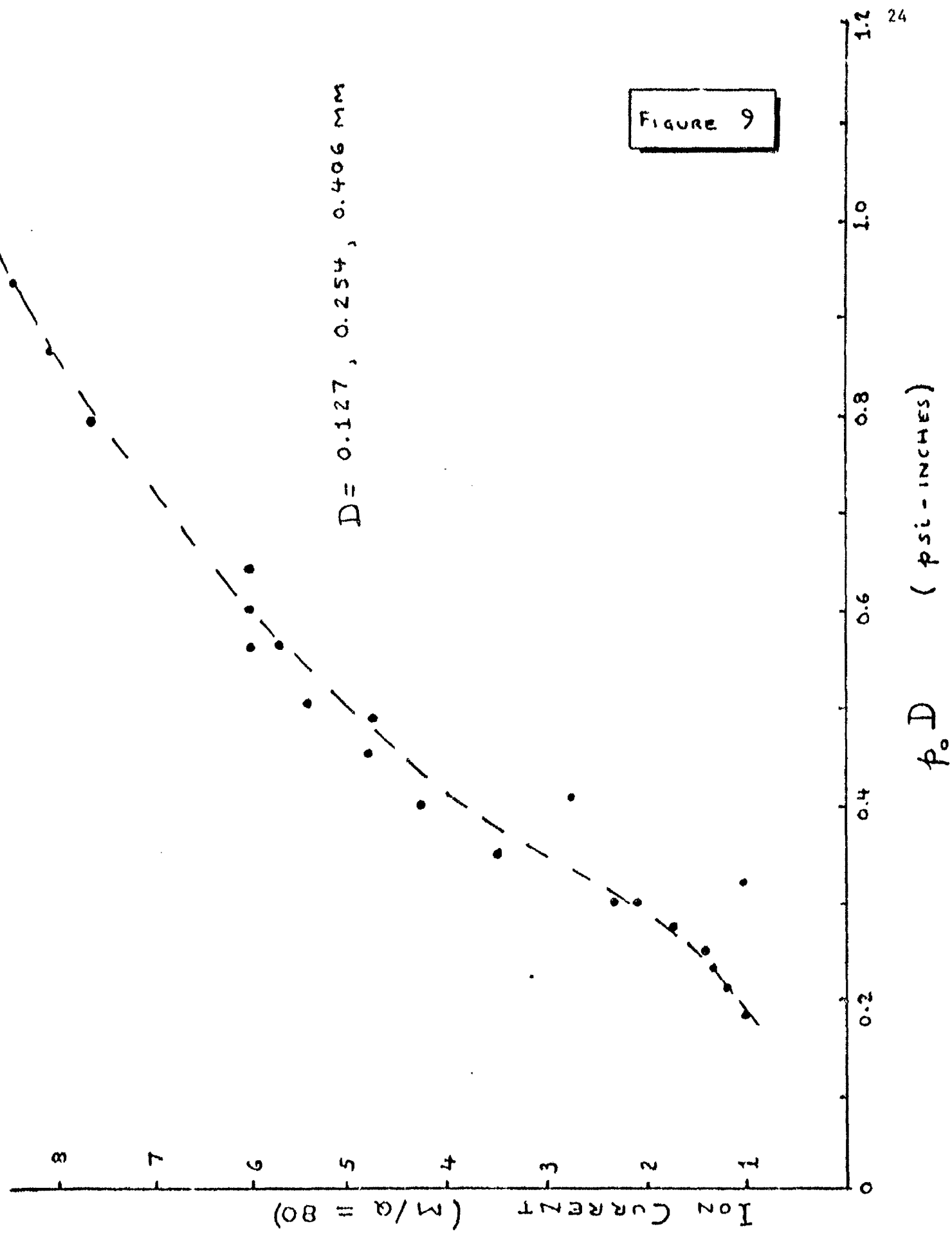


FIGURE 9



III.E: CALCULATED DIMER CONCENTRATIONS

Since the success of our program hinged on the validity of earlier estimates of argon dimer concentrations in the free expansion,^[40] we recalculated the mole fraction per unit number density as a function of the translational temperature T_{\perp} in the beam. Calculations for both homonuclear and heteronuclear inert-gas diatomics were performed with the method of Strogryn and Hirschfelder;^[41] metastable contributions to the mole fraction were included under an assumed Lennard-Jones interaction. The conservative experimental parameters used are listed in Table III.^[42]

As a guide, we note that, although T_{\perp} will freeze out at about 10K in our system, T_{\perp} will go to lower temperatures. The results, given in Figures 10 through 12, confirmed our original rough estimates and indicated that homonuclear and heteronuclear dimers (and so excimers) of Xe, Kr, and Ar should be most easily studied.^[43]

TABLE III: LENNARD-JONES PARAMETERS [42]

Based on conservative choices of experimental values.

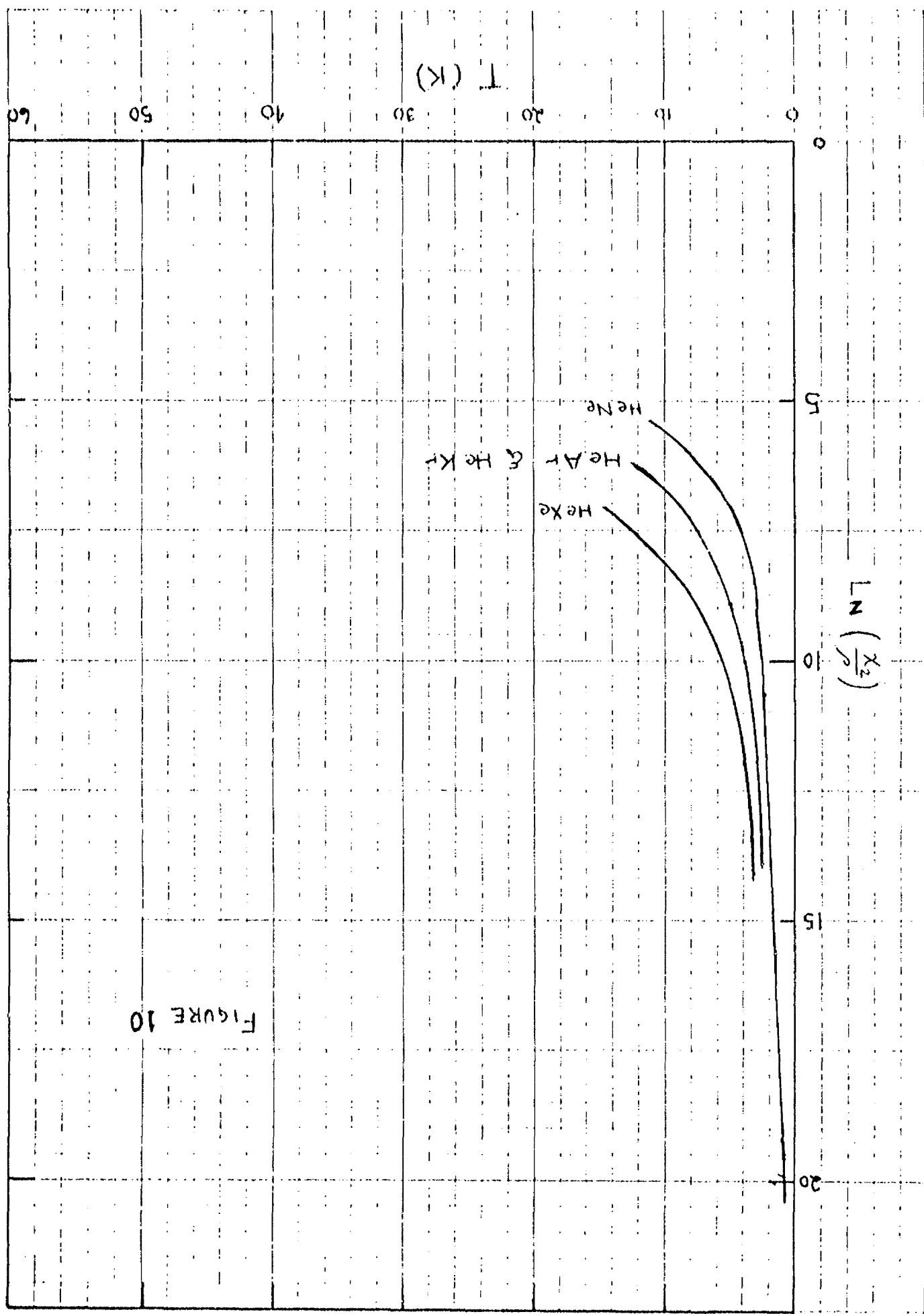
DIMER	σ [10 ⁻⁸ cm]	ϵ [10 ⁻¹² erg]	REFERENCES
He-He	2.65	23.5	J. Farrar et. al. J. Chem. Phys. 56, 5801 (1972)
Ne-He	23	2.64	D. Konowalow et. al. J. Chem. Phys. 57, 4375 (1972) R. Van Heijningen et. al. Physica (UTR) 37, 1 (1968)
Ar-He	34	2.93	D. Konowalow et. al. J. Chem. Phys. 57, 4375 (1972) R. Van Heijningen et. al. Physica (UTR) 38, 1 (1968)
Kr-He	33	3.13	R. Van Heijningen et. al. Physica (UTR) 38, 1 (1968)
Xe-He	59	3.32	R. Van Heijningen et. al. Physica (UTR) 38, 1 (1968)
He-Ne	63	2.73	P. Siska et. al. J. Chem. Phys. 55, 5762 (1971)
Ar-Ne	3.08	80	R. Van Heijningen et. al. Physica (UTR) 38, 1 (1968) J. Kestin et. al. J. Chem. Phys. 53, 3773 (1970) J. Parson et. al. J. Chem. Phys. 53, 2123 (1970)

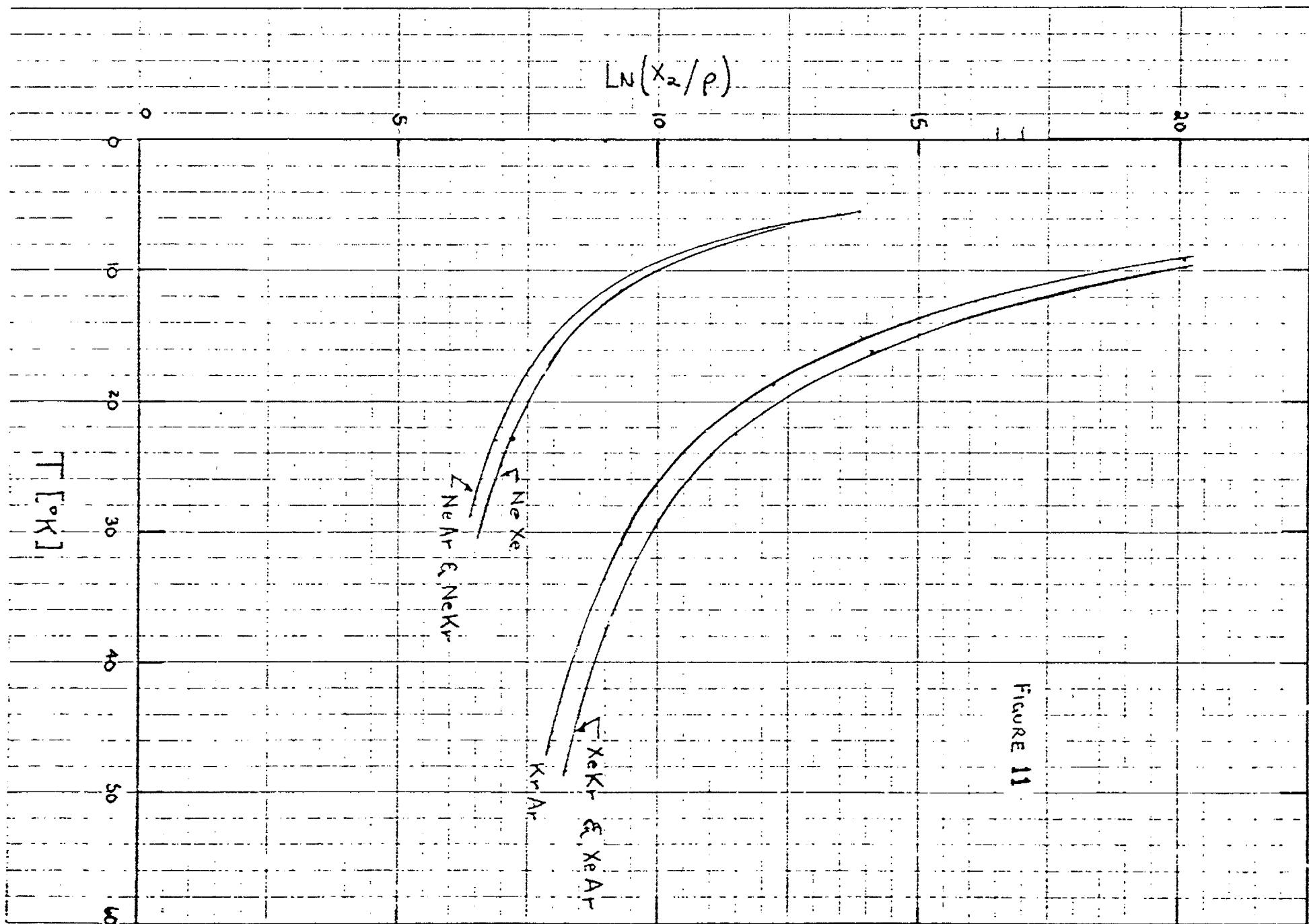
Table III (Continued)

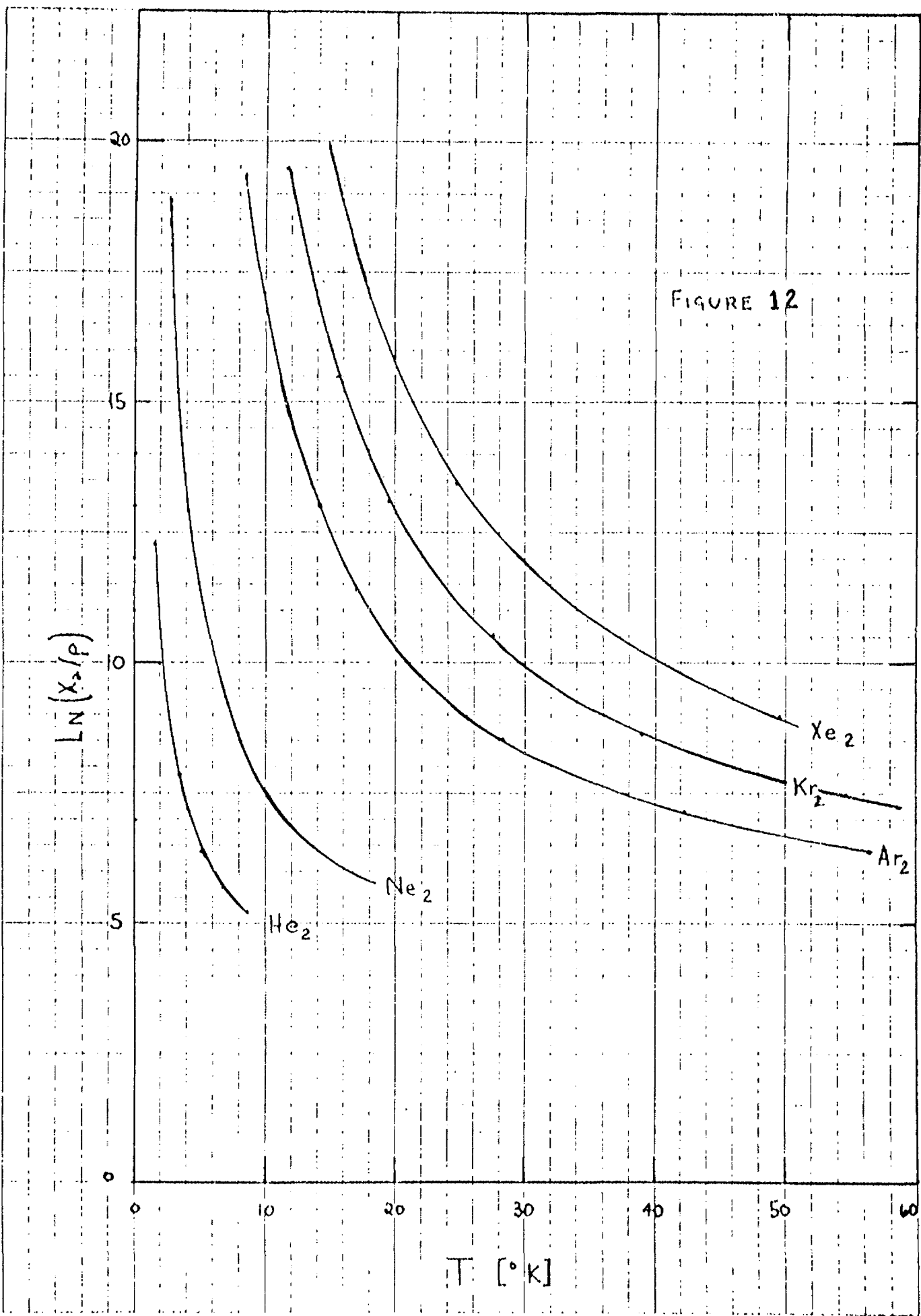
DIMER	σ [10 ⁻⁸ cm]	ϵ [10 ⁻¹² erg]	REFERENCES
Kr-Ne	3.16	80	R. Van Heijningen et. al. Physica (UTR) 38, 1 (1968) J. Parson et. al. J. Chem. Phys. 53, 2123 (1970) J. Kestin et. al. J. Chem. Phys. 56, 4086 (1972)
Xe-Ne	79	3.44	R. Van Heijningen et. al. Physica (UTR) 38, 1 (1968) J. Parson et. al. J. Chem. Phys. 53, 2123 (1970)
Ar-Ar	195	3.32	J. Parson et. al. J. Chem. Phys. 56, 1511 (1972)
Kr-Ar	214	3.41	J. Kestin et. al. J. Chem. Phys. 53, 3773 (1970) J. Parson, et. al. J. Chem. Phys. 53, 3755 (1970)
Xe-Ar	236	3.60	R. Van Heijningen et. al. Physica (UTR) 38, 1 (1968) J. Parson et. al. J. Chem. Phys. 53, 3755 (1970)
Kr-Kr	270	3.48	D. Konowalow et. al. J. Chem. Phys. 57, 4375 (1972)
Xe-Kr	223	3.82	R. Van Heijningen et. al. Physica (UTR) 38, 1 (1968)
Xe-Xe	342	3.85	J. Kestin et. al. J. Chem. Phys. 56, 4119 (1972). G. Davis B. Davis B.J. Chem. Phys. 57, 5098 (1972).

Based on a literature search reported by Y. Kim and R. Gordon, J. Chem. Phys., 61, 1 (1974).

FIGURE 10







III: THE STATUS OF THE APPARATUS

The status of our research is mirrored in the status of our apparatus. For purposes of design, procurement, and construction, our experimental system was divided into 25 interrelated subsystems, A through Y (See Figure 13). The following subsystems have been completed:

A through D,

G through P,

R and S, and

U through Y.

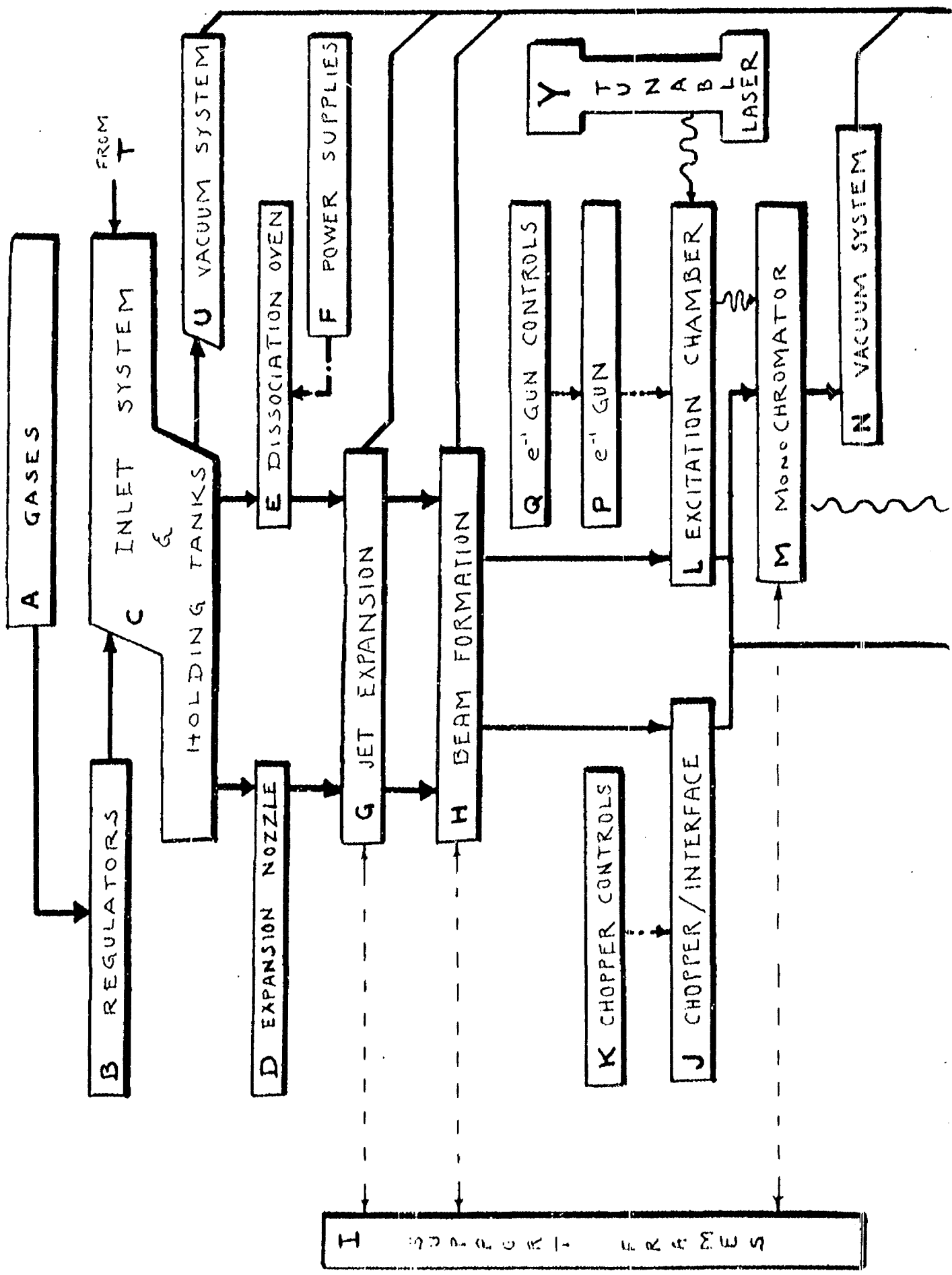
The dissociation oven and related power supplies, E and F, were dropped from the project, when we were directed to discontinue work on inert-gas halides and oxides. Electron-gun controls, Q, are actually in use; only the pulse circuitry (for future excimer-lifetime measurements) remains to be assembled. The gas recovery system, T, will be assembled when work on Xenon systems begins.

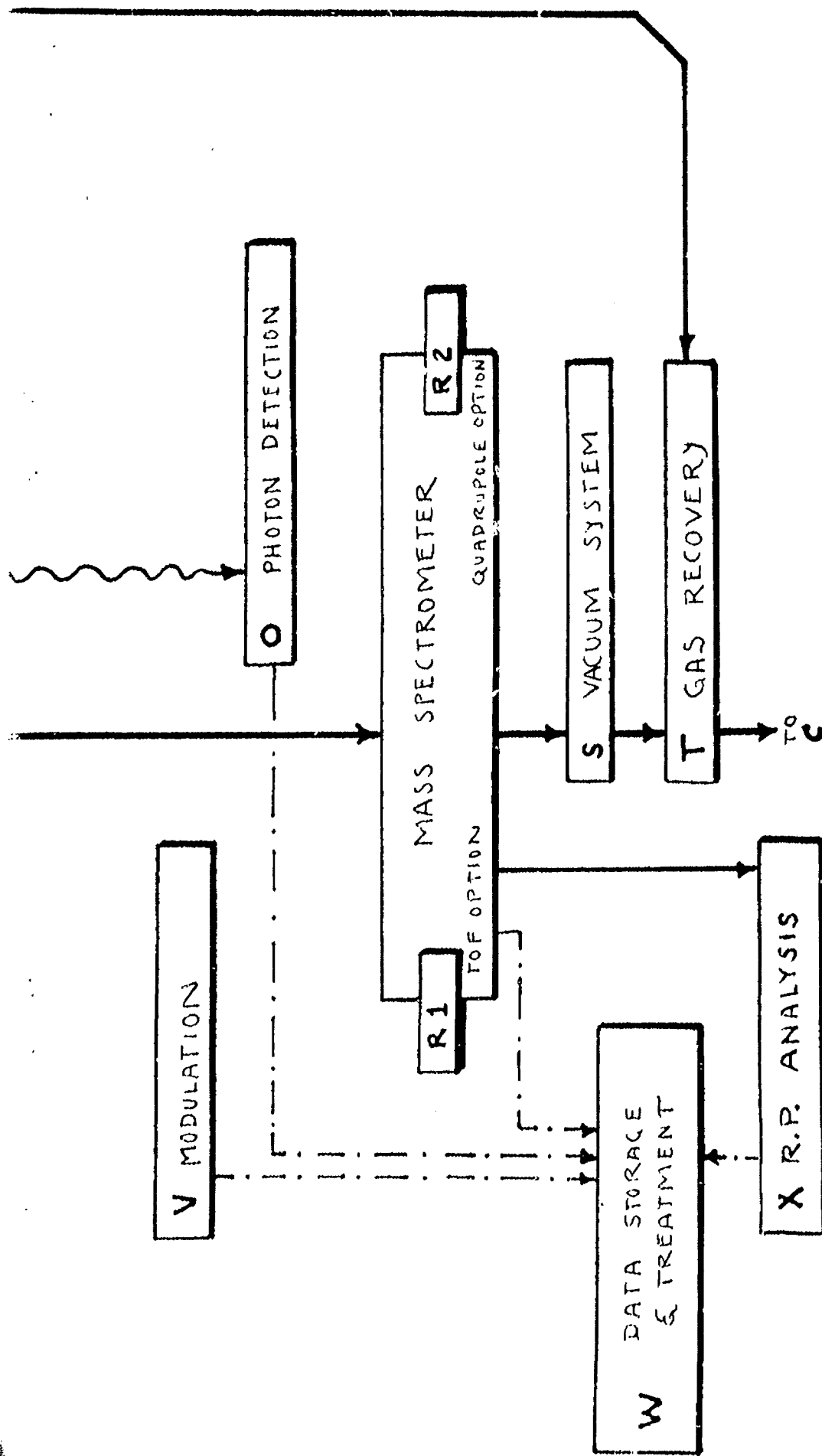
Functionally, our experimental system is composed of the following major units:

1. The Cluster-Molecular Beam source of van der Waals dimers;
2. The Mass-Spectrometer Monitor of molecular beam composition;
3. The Low-energy Electron-Beam Source of excimers;
4. The Excimer Monitoring System (vacuum-UV to visible detection and photon counting);
5. A Tunable Laser for absorption measurements.

The cluster-molecular beam is shown in Figures 14 and 15; its performance has been discussed in section II of this report.

BLOCK DIAGRAM





BLOCK DIAGRAM
FIGURE 13

III.A: MASS SPECTROMETERS

Two options are available for the measurement of molecular beam composition: time-of-flight or quadrupole mass spectrometry.

A Bendix Model 12 TOF mass spectrometer was obtained under a Loan Contract from USEPA, Cincinnati, but has been dedicated to this project via an Excess Property Transfer. This instrument, originally designed by the principal investigator in 1960, is now a fully functioning mass spectrometer. It has a sensitivity of 0.1 amp per torr and a unit mass resolution of 300 d/e⁻.

Our quadrupole option was, at first, based on a Varian RGA of uncertain vintage and model number, obtained on loan from NASA, Langley Research Center. When operational, it was shown to detect partial pressures to 5×10^{-11} torr with a unit resolution of 50 d/e⁻ in the mass range from 10 to 250 d/e⁻. Circuitry to expand the mass range to 600 d/e⁻ was built but never incorporated; once the instrument's performance was known, it was obvious that the mass-range expansion would deteriorate the resolution to less than 35 d/e⁻.

To optimize dimer production in the molecular beam, we have to manipulate the cluster size distribution. This, in turn, requires unit resolution of 600; the tetramer $^{134}\text{Xe}_4$, for example, has a mass of 536 d. A used AET Model 250 quadrupole mass spectrometer was obtained; both the quadrupole head and its electronics were modified. In its present configuration, this instrument has a base-line resolution of 600 d/e⁻.

Despite the seemingly large number of publications in this area, mass spectrometry of cluster beams is in its infancy. The principle problem

is the lack of established criteria for cluster-size distributions. In addition, ionization energetics show anomalies.^[44] The use of combined (retarding-potential) energy and mass analyses in alternate cycles should provide a new standard for size-distribution measurements. A retarding-potential analyzer has been developed for use with our TOF spectrometer; it mounts in line with the molecular beam, but is downstream of the mass-spectrometer electron beam. (See Figure 5.) This approach to cluster-beam spectrometry should prove especially useful in our studies of heteronuclear excimers.

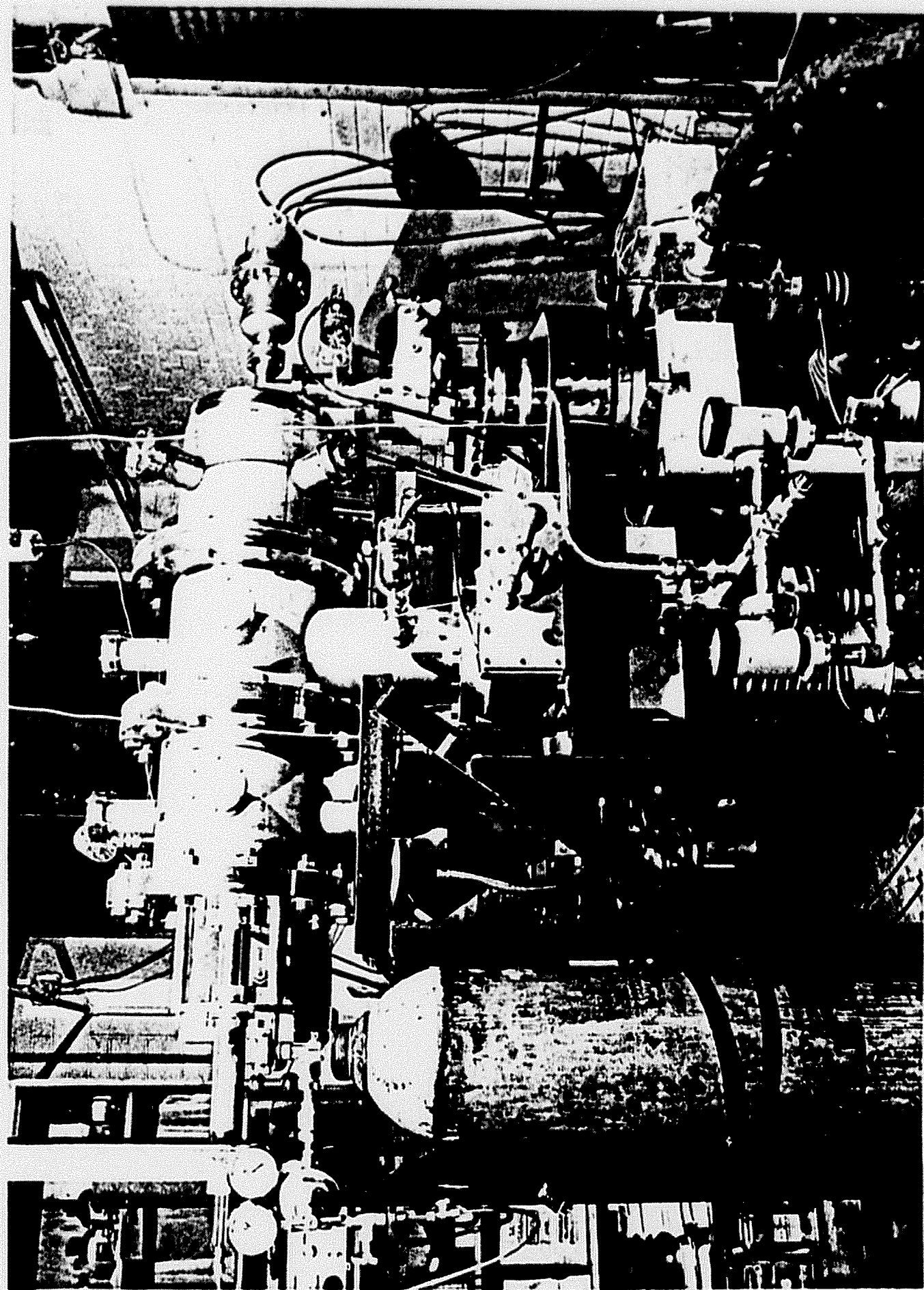


FIGURE 14: CLUSTER BEAM SYSTEM WITH QUADRUPOLE MASS SPECTRUM

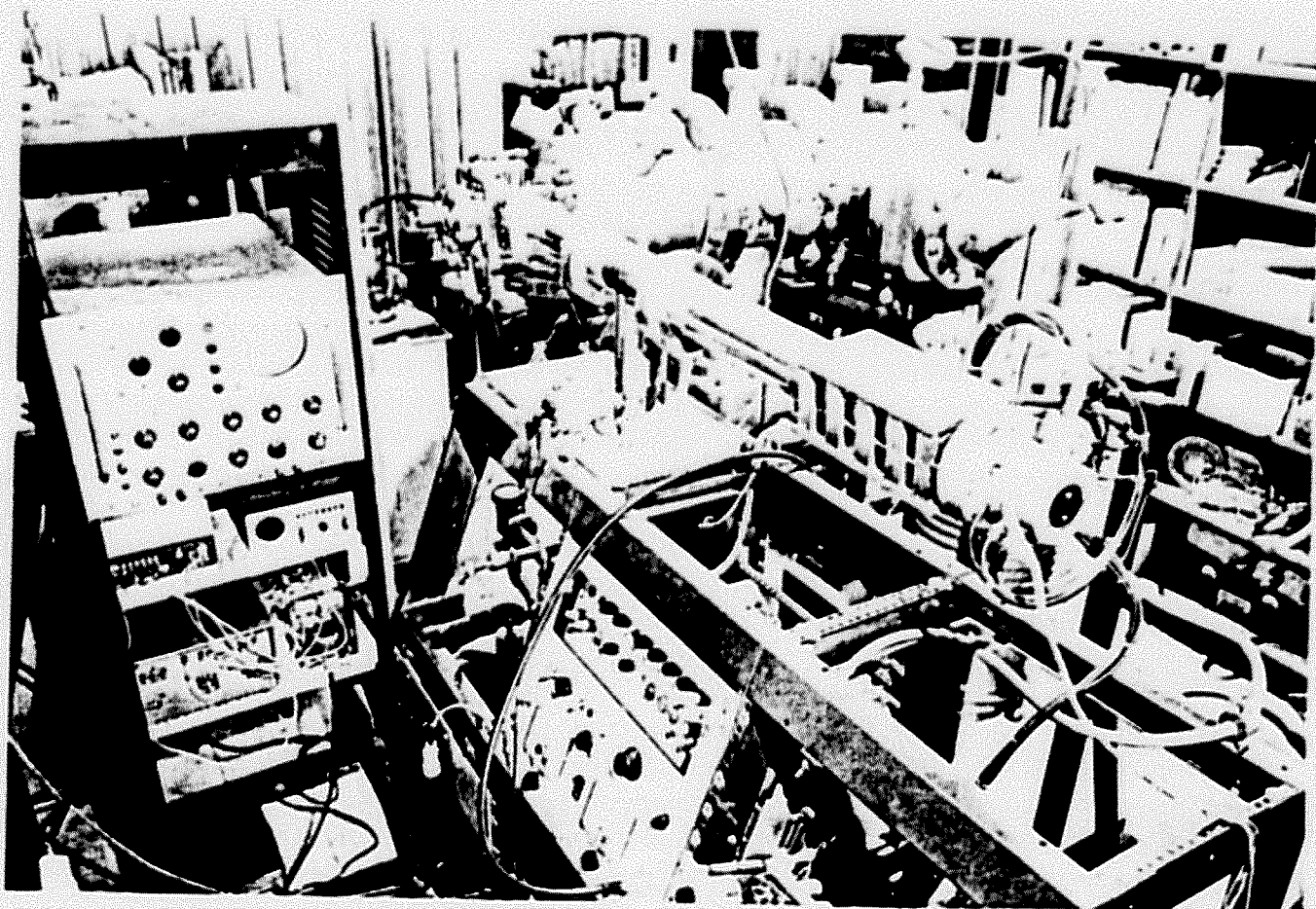


FIGURE 15:

CLUSTER BEAM WITH T.O.F. MASS SPECTROMETER.

III.B: EXCITATION ELECTRON GUN

During development of an acceptable electron gun for our excimer studies, continual difficulties arose. The incompatible criteria of high beam current and low energy bandpass required a working compromise. In retrospect, we spent too much time seeking this compromise.

The first gun, shown in Figure 16, used ribbon filaments and cathode-ray-tube optics; it satisfied neither of the above-mentioned criteria. Successive designs employed directly-heated wires or indirectly-heated cathodes with an evolving set of electron optics. For narrow bandpass, beam currents were still restricted to less than 100 μ A.

Figure 17 illustrates the newly completed "final" version. Using a tungsten spiral filament with deceptively simple electron optics, this gun has produced beam currents of over 500 μ A at electron energies of 50 eV. The electron beam is electrostatically focussed with optics designed by field graphing. All gun elements, including the electron trap, are mounted to a single-piece, stainless steel frame. Electrical insulation is provided by the material "Vespel", an experimental polymer developed by Dupont, which is easily machined and is stable at the high temperatures surrounding the filament.

Grids have been included which, with RPD analysis,^[46] should allow an excitation energy resolution of ≥ 0.02 eV.

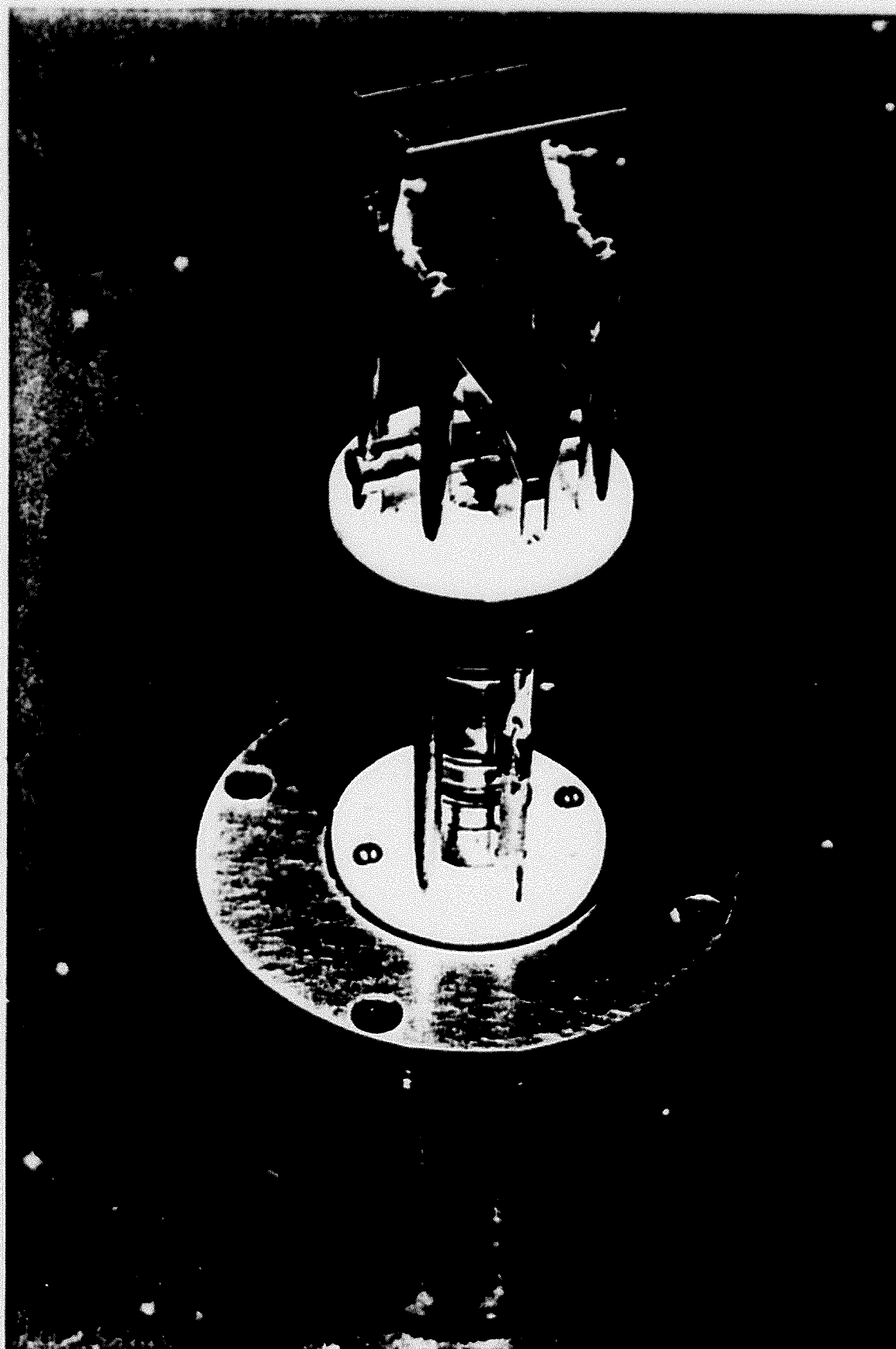


FIGURE 16: FIRST ELECTRON GUN

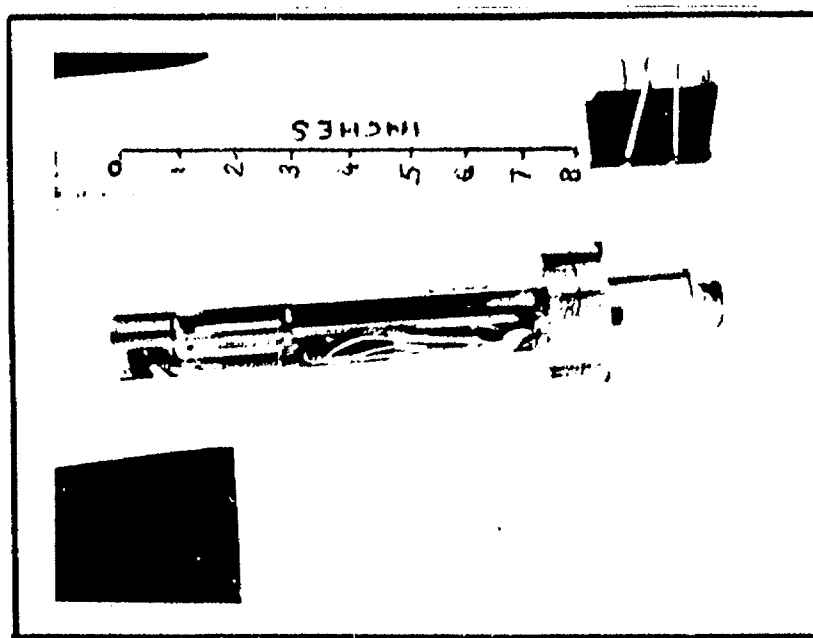
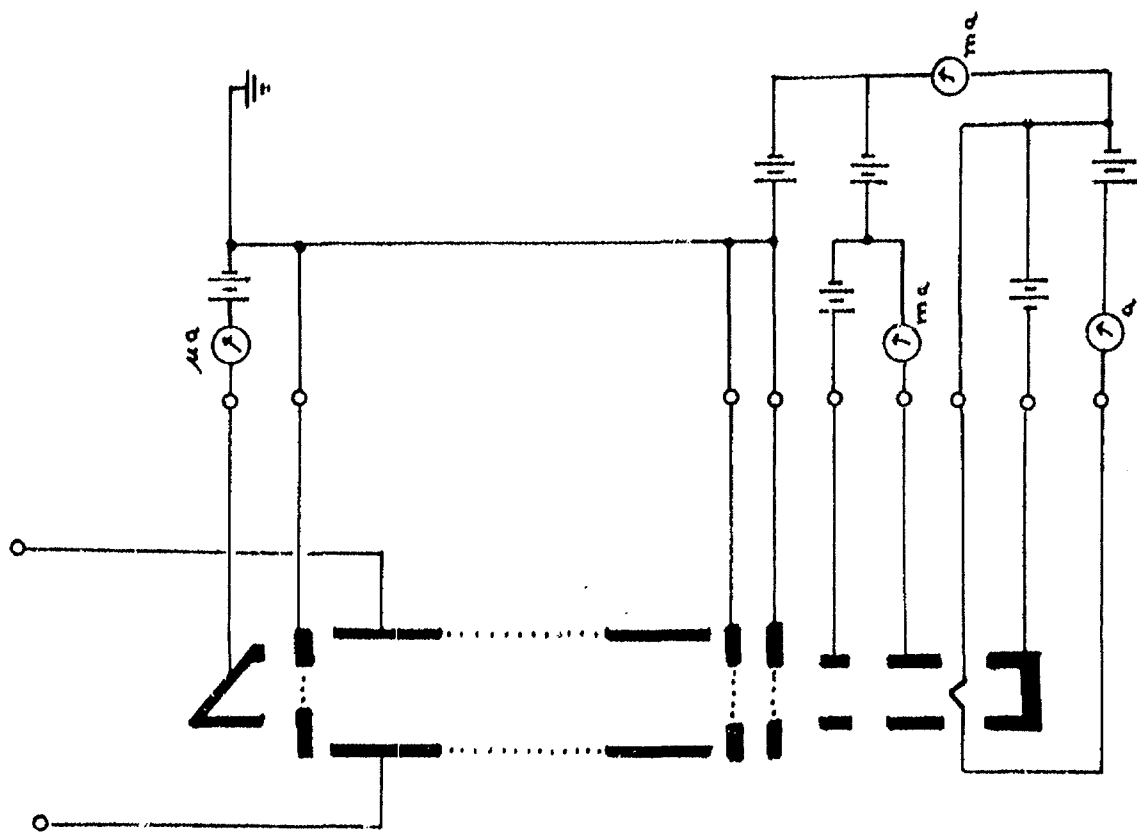


FIGURE 17: "Final" Electron Gun.

III.C: PHOTON DETECTION

The photon-detection system, required to monitor excimer emission, consists of the following major components: a Minuteman Labs Model 302-VM scanning Vacuum-UV/Visible monochromator; a Model 1109 photon counter and a Model 1121 amplifier-discriminator from Princeton Applied Research; an EMI-9635QB photomultiplier; a Products For Research TE-104 pm chamber; and a Galileo CEM 4000 electron multiplier. Since this type of system was new to the principal investigator, its design was given top priority; moreover, the components had the longest lead times of the commercial equipment required.

A Chromatix Model CMX-4 flash-excited, tunable dye laser was obtained for excimer-absorption studies. With spectroscopic detection and laser excitation, the excimer formation chamber is the site of the confluence of three beams: the molecular, excitation-electron, and laser beams. In addition, the photon-detection system must focus on the volume of intersection these three beams.

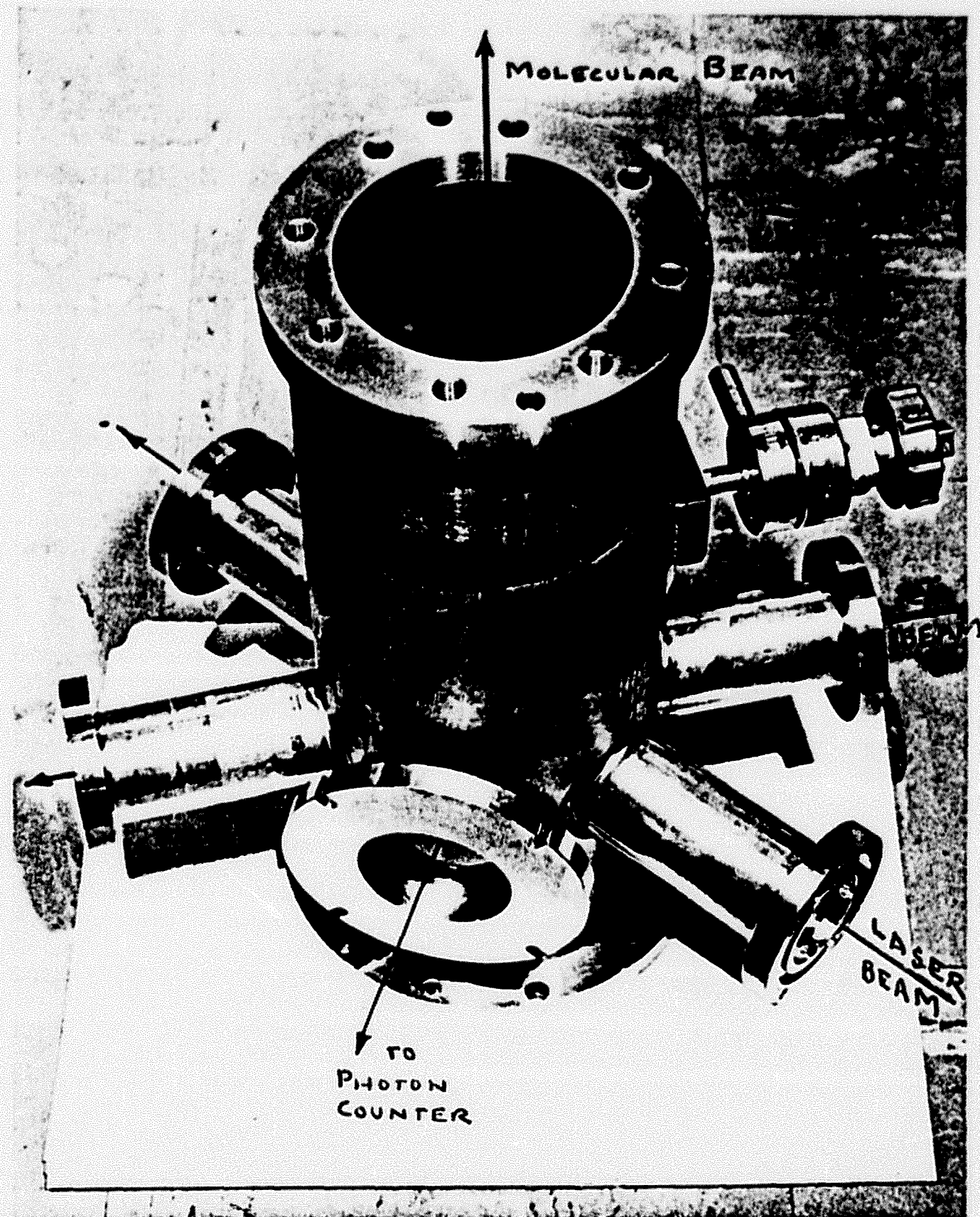


FIGURE 18: BEAM EXCITATION CHAMBER

IV: FORMATION OF EXCIMERS

According to the proposed mechanism (See Figure 1), excimers and exciplexes will be formed by electron bombardment of van der Waals complexes. Since resonant-electron pumping is a Franck-Condon process, vibrotational states must exist near the dissociation limit of AB^\ddagger , i.e. at the internuclear configuration of the van der Waals complex. This requirement will surely be satisfied. For example, Li and Stwalley found such states in the spectrum of Mg_2 at internuclear separations of 10 angstroms^[45] (where the difference between the electronic energy and dissociation limit is about 0.05 ev). The potential well for Xe_2^* is about 1.0 ev.^[1]

The formation rate for AB^\ddagger is given by

$$\frac{d[AB^\ddagger]}{dt} = k [AB] N_e,$$

where N_e is the number of electrons in the volume of intersection of the dimer and electron beams. With an electron-excitation cross section of $2 \times 10^{-18} \text{ cm}^2$, rate constant k takes a value of $3.6 \times 10^{-10} \text{ cm}^3/\text{electron}/\text{second}$. For Xe_2^\ddagger , we should form more than 10^9 excimers per second.

If we assume a radiative lifetime of 20 ns for AB^\ddagger and a reasonable value for the de-excitation cross section,^[48] then less than one percent of our excimers will be vibrotationally excited. However, our objective is, in part, to discover bound-free systems with radiative lifetimes longer than 20 ns.

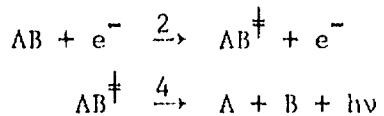
The experimental program, as first proposed, involved four basic classes of measurement: spectra, excitation cross sections, reactive cross sections, and lifetimes. As our work progressed, two additional measurement capabilities were built into our apparatus: photofontization and resonant self absorption.

IV.A: VISIBLE TO VACUUM-ULTRAVIOLET SPECTRA

Since emission spectra should help in the characterization of potential new laser materials, we plan to monitor the visible to vacuum-ultraviolet regions of the spectrum for each species studied. Low-pressure studies should yield well-resolved spectra,^[2,49] but photon-counting will be employed when required.

IV.B: ELECTRON EXCITATION CROSS SECTIONS

The cross-sections for electron-beam formation of excimers and exciplexes can be deduced from steady-state emission intensities, provided that the excitation chamber is at very low background pressures.



At steady-state, the emission of AB^\ddagger is proportional to the rate of reaction (2); if the electron-beam current is directly monitored, while the AB dimer concentration is measured with the mass spectrometer, then the rate constant (and so the cross-section) for (2) can be found as a function the electron energy. Absolute cross-sections may have large uncertainties, but relative cross sections will be more accurately determined; it may be necessary to extrapolate measured cross-sections to their values at zero background pressure.

IV.C: REACTIVE CROSS SECTIONS

Once the cross-sections for excimer formation have been determined, total cross-sections for quenching reactions (collisional de-excitation and dissociation) can be determined. By the simple procedure of varying background gas pressure and composition under the conditions of steady-state excimer formation, data leading to reactive cross sections can be obtained. Again, it is relative cross-sections which can be most accurately determined.

IV.D: LIFETIMES

Since some of the new excimer or exciplex systems under study will have lifetimes on the order of collision times, a first probe of lifetime is provided by the dependence of emission spectra on variations in background pressure. However, actual lifetime measurements will involve relaxation studies with pulsed electron-beam excitation and time-delayed photon counting.

Using recently available electron-bombardment-semiconductor devices,^[50] we have generated very fast-risetime, high-energy pulses for the measurement of lifetimes shorter than 3 ns.^[51] With this ability to measure lifetimes to 2 ns, we can now probe kinetic complexities; for example, the existence of two different lifetimes (5 and 40 ns, respectively) for singlet and triplet rare-gas excimer manifolds^[52] can be directly confirmed. The lifetime measurements are the most difficult experiments planned in this research.

IV.E: RESONANT SELF-ABSORPTION

In high-pressure lasers, resonant self-absorption of lasing emission could lead to a serious depletion of excimer (through the formation of more-highly-excited states). To study these processes, the following experiment, employing a tuned laser, was proposed. Upward-bound optical transitions induced by a laser (tuned near the excimer's lasing frequency) would be monitored via emissions from the more-highly-excited states.

As noted in the following section, this experiment is feasible only because resonant-absorption cross-sections for visible light are extremely large. Measurements will be complicated if the potential energy minima

for both excimer and van der Waals dimer occur at the same internuclear separation. But even this unusual case could be revealed in laser excitation studies of the ground-state dimer.

IV.F: UPWARD-BOUND TRANSITIONS

Upward optical transitions (process 6 in Figure 1) can be studied via the emission from the more-highly-excited states formed; this is a consequence of the extremely large cross-sections for resonant absorption of visible light.

If τ is the radiative lifetime of the excimers formed by electron-beam excitation, then the number of excimers, N^{\ddagger} , present after a time t is

$$N^{\ddagger} = \frac{dN^{\ddagger}}{dt} \left\{ 1 - \exp\left(-\frac{t}{\tau}\right) \right\} \tau ,$$

where dN^{\ddagger}/dt is the steady-state excimer production rate, 10^9 excimers/sec. If τ is 20 ns, then

$$N^{\ddagger} = 20 \left\{ 1 - \exp\left(-\frac{t}{\tau}\right) \right\} .$$

Let P be the number of photons required to excite every excimer by resonant absorption; then

$$P = \frac{N^{\ddagger} A}{\sigma_{\text{res}}} ,$$

where A is the area of the molecular beam ($\approx 0.01 \text{ cm}^2$), and σ_{res} is the cross-section for resonant absorption. The latter quantity is proportional to the square of the wavelength for the transition; for a Breit-Wigner lineshape:

$$\sigma_{\text{res}} = 0.477 \lambda_0^{-2}$$

For $\lambda_0 = 5000 \text{ angstroms}$,

$$P = 4 \times 10^8 \left\{ 1 - \exp\left(-\frac{t}{\tau}\right) \right\} \approx 1.6 \times 10^8 \text{ photons}$$

This corresponds to a laser power of 64 mw; the Chromatix Model CMX-4, the laser available for this research, is capable of 3 kw peak power at 90 mw average power, when operating at 30 pulses per second.

IV.G: PHOTOTIONIZATION OF EXCITED STATES

Another important, but difficult, class of experiment is possible because a mass spectrometer is being used to monitor molecular beam composition. See Figure 19.

With its electron beam off, the mass spectrometer acts as a passive ion detector; consequently, dimer ions, AB^+ , produced by photoionization of AB^* can be detected. Structure in the photoionization efficiency curve for AB^+ which is induced by the excitation electron beam, can immediately be interpreted in terms of the photoionization of the excited states of the dimer. While photon counting of excimer fluorescence indicates the steady-state excimer population, ion counting measures the steady-state photo-ion current. By monitoring laser intensity, we can then determine photoionization cross sections.

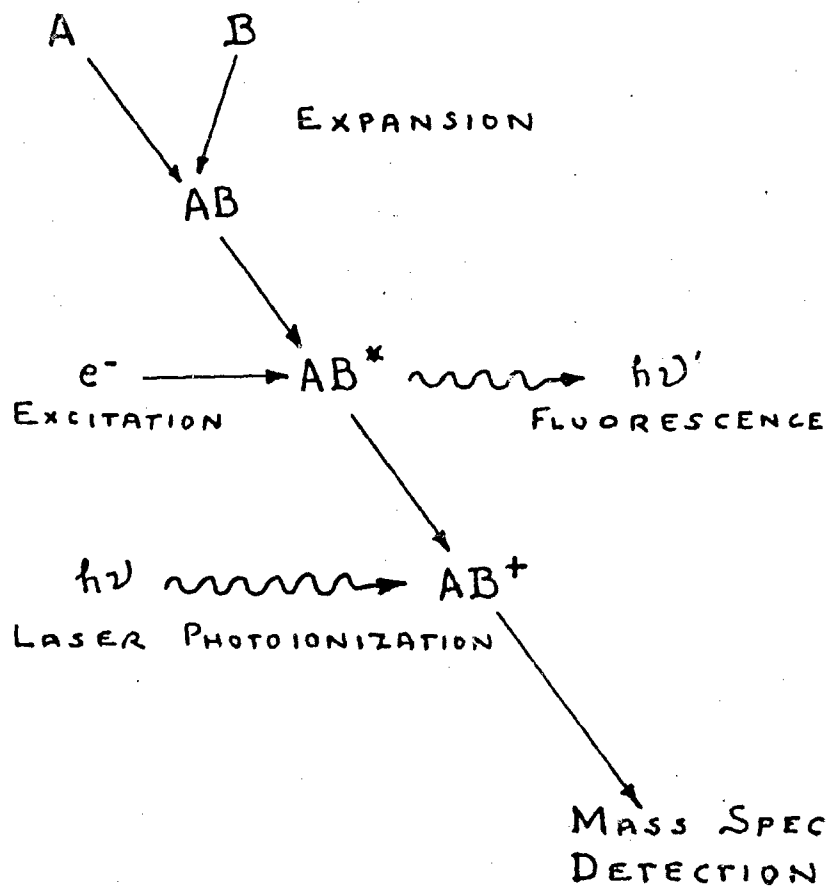


FIGURE 19:
PHOTO-IONIZATION OF EXCITED STATES

V: MERCURY & MERCURY-INERT GAS SYSTEMS

There has been some interest in metal vapor excimer systems as candidates for lasers.^[53] As an example, the lowest electronic levels in Group IIB elements are metastable with lifetimes from 0.1 to 1.0 microsecond.

The ground-state mercury dimer can be produced in the free expansion. There are, however, problems unique to metal-vapor work which must be solved: in particular the maintainence of high purity, and the generation of high vapor pressures. In this work, an inert-gas sweep-out technique was planned for the formation of mercury-inert gas dimers in the free-jet expansion; Hg_2 would also be formed. Our study did not go beyond the planning stage, although a heated sweep-out source was designed.

VI: CALCULATIONS OF POTENTIAL ENERGY CURVES

With the study of the fluorescence and product energy distribution of HeI_2 , the use of van der Waals_{^{molecules}} as photochemical prototypes has now been recognized; [54] this species, however, is relatively long-lived (10^{-7} sec) and, at the pressures used, reactive quenching has dominated observed kinetics. A key goal of the low-pressure approach has been the separation of quenching kinetics from formation and radiative-dissociation kinetics; in particular, we have been interested in excimers and exciplexes of heteronuclear van der Waals clusters - about which little is known regarding stability, or formation and ionization kinetics. It had been hoped to develop an in-house theoretical expertise on such systems and to compute ground-state potential energy curves for heteronuclear (as well as homonuclear) inert gas diatomic molecules and ions.

Some preliminary calculations were included in earlier progress reports; they deserve little further comment, since the theoretical calculations never really got off the ground. The principal investigator is considering the initiation of such calculations himself, they would be useful in setting limits on the concentrations of species which either can be formed in the jet expansion, or can be detected mass spectrometrically.

VII: REFERENCES

1. (a) F. K. Boutermans, *Helv. Phys. Acta* 33, 933 (1960);
(b) C. K. Rhodes, *IEEE J. Quantum Elect.* QE-10, 153 (1974).
2. (a) C. K. Rhodes & P. W. Hoff, UCRL-74922 (Aug. 3, 1973);
(b) H. T. Powell, J. R. Murray & C. K. Rhodes, *Appl. Phys. Lett.* 25, 730 (1974);
(c) J. E. Valazco & D. W. Setzer, *J. Chem. Phys.* 62, 1990 (1975).
3. G. A. West and M. J. Berry, *J. Chem. Phys.* 61, 4700 (1974).
4. (a) W. Forst, "Theory of Unimolecular Reactions," (Academic Press, 1973);
(b) E. E. Nikitin, in "Chemische Elementarprozesse", Edited by H. Hartmann (Springer-Verlag, Berlin, 1968), p. 43.
5. (a) T. A. Milne and F. T. Greene, *J. Chem. Phys.* 47, 4095 (1967);
(b) P. P. Wegener and J. Y. Parlange, NATO AGARD Publication AD 658-781, Vol. II, p. 607 (1967);
(c) S. S. Lin, *Rev. Sci. Instr.* 44, 516 (1973);
(d) Otto F. Hagen, in "Molecular Beams & Low-Density Gasdynamics", Edited by P. P. Wegener (Marcel Dekker, Inc., N.Y., 1974), p. 93;
(e) R. E. Smalley, D. H. Levey and L. Wharton, *J. Chem. Phys.* 64, 3266 (1976);
(f) C. B. Cosmovici, et. al., *Rev. Sci. Instr.* 47, 667 (1976).
6. H. W. Liepmann and A. Roshko, "Elements of Gas Dynamics," (John Wiley and Sons, N.Y., 1957).
7. G. Sanzone, "The Mass Spectrometric Sampling of Shock-Tube Flows For the Study of High-Temperature Reaction Rates," Ph.D. Thesis, Univ. of Illinois (1969).

8. J. B. Anderson, R. P. Andres, and J. B. Fenn, *Adv. Chem. Phys.* X, 275 (1966).
9. V. K. Bier and B. Schmidt, *Z. Angew. Phys.* 13, 493 (1961).
10. S. Crist, P. M. Sherman, and D. R. Glass, *AIAA J.* 4, 68 (1969).
11. H. Ashkenas and F. S. Sherman, in "Rarefied Gas Dynamics," Supplement 3, Vol. 2, (Academic Press, N.Y., 1966), p. 84.
12. A. Kantrowitz and J. Grey, *Rev. Sci. Instr.* 22, 328 (1951).
13. H. M. Parker, A. R. Kuhlthau, R. N. Zapata and J. E. Scott, Jr., in "Rarefied Gas Dynamics," (Pergamon Press, London, 1960), p. 69.
14. D. Beck and R. Morganstern, *Diplomarbeit*, Freiburg Univ. (1967). Cited in reference 17.
15. R. J. Gordon, Y-T. Lee, and D. R. Herschbach, *J. Chem. Phys.* 54, 2393 (1971).
16. E. W. Becker and W. Henkes, *Z. Physik* 146, 320 (1956).
17. J. B. Anderson and J. B. Fenn, *Phys. Fluids* 8, 780 (1965).
18. B. B. Hamel, *AIAA J.* 2, 1047 (1964).
19. R. H. Edwards and H. K. Cheng, *AIAA J.* 4, 558 (1966).
20. B. B. Hamel and D. R. Willis, *Phys. Fluids* 9, 829 (1966).
21. E. P. Muntz, in "Rarefied Gas Dynamics," Supplement 4, Vol. 2 (Academic Press, N.Y., 1967), p. 1257.
22. J. E. Scott and J. A. Phipps, in "Rarefied Gas Dynamics," Supplement 4, Vol. 2 (Academic Press, N.Y., 1967), p. 1337.
23. S. S. Fischer, *Ph.D. Thesis*, Univ. of California, Los Angeles (1967).
24. D. R. Willis and B. B. Hamel, in "Rarefied Gas Dynamics," Supplement 4, Vol. 1 (Academic Press, N.Y., 1967), p. 837.
25. G. Sanzone and R. L. Belford, *Proc. 18th Annual Conf. Mass Spectrom. & Allied Topics*, June, 1970, San Francisco, Calif., p. 8294.

26. A. A. Stepchko, *ARS J.*, 30, 695 (1960).
27. T. A. Milne and F. T. Greene, *J. Chem. Phys.* 47, 4095 (1967).
28. P. P. Wegener and J. Y. Parlange, *NATO AGARD Publication AD* 658-781, Vol. II, p. 607 (1967).
29. K. Bier and O. Hagen, in "Rarefied Gas Dynamics," Supplement 3, Vol. 2 (Academic Press, N.Y., 1966), p. 260.
30. P. Kebarle, *Adv. Chem.* 72, 24 (1968). "Mass Spectrometry in Inorganic Chemistry," (ACS, Washington, D.C.). (Also see Ref. 27, above).
31. T. A. Milne and F. T. Greene, *Adv. Chem.* 72, 64 (1968).
32. R. E. Leckenby and E. J. Robbins, *Proc. Roy. Soc.* 291, 389 (1966).
33. E. Buluggin and C. Foglia, *Chem. Phys. Letters* 1, 82 (1967).
34. D. E. Stogryn and J. O. Hirschfelder, *J. Chem. Phys.* 31, 1531 (1959); 32, 942 (1960).
35. S.-S. Lin, *Rev. Sci. Instr.* 44, 516 (1973).
36. F. T. Greene and T. A. Milne, *Advan. Mass Spectrom.* 3, 841 (1966).
37. "The Formation & Study of Exciplex Systems: A Low-Pressure Approach," Quarterly Progress Report No. 1 (Dec. 1, 1975 to Feb. 29, 1976). USERDA-COO-2810-2.
38. H. Askenas & F. S. Sherman, in "Rarefied Gas Dynamics, 4th Symp." (Academic Press, N.Y., 1966).
39. (a) T. A. Milne & F. T. Greene, *Adv. Chem.* 72, 64 (1968);
(b) J. P. Vallenau & J. M. Deckers, *Can. J. Chem.* 43, 6 (1965);
(c) Also see the many articles on this subject in the supplements to "Rarefied Gas Dynamics".
40. "The Formation and Study of Exciplex Systems: A Low-Pressure Approach", Progress Report No. 2 (Mar. 1 to May 31, 1976). USERDA-COO-2810-3.

41. D. E. Stogryn and J. O. Hirschfelder, *J. Chem. Phys.* 31, 1531 (1959).
42. Y. Kim and R. Gordon, *J. Chem. Phys.* 61, 1 (1974).
43. R. W. Mattozzi, C. D. Williams, and G. Sanzone, "The Formation of van der Waals Dimers in Cluster Beams," Presented at the 28th Southeastern Meeting of the A.C.S., Tampa, Fla. (Oct., 1976).
44. P. E. Wegener, ed., "Molecular Beams and Low Density Gasdynamics," (Marcel Dekker, N.Y., 1974).
45. K. C. Li and W. C. Stwalley, *J. Chem. Phys.* 59, 4423 (1973).
46. (a) R. E. Fox, W. M. Hickam, D. J. Grove, and T. Kjeldaaas, Jr., *Rev. Sci. Instr.* 26, 1101 (1955);
(b) G. G. Cloutier and H. I. Schiff, *Adv. Mass Spectrom.* Vol. I, 473 (Pergamon Press, N.Y., 1959).
47. M. J. Seaton, In "Atomic & Molecular Processes," D. R. Bates, ed., (Academic Press, N.Y., 1962).
48. (a) D. J. Bradley, M.H.R. Hutchinson, and H. Koetsier, *Optics Comm.* 1, 187 (1973);
(b) A. B. Callear and G. J. Williams, *Proc. Roy. Soc. (London)*, 289, 2158 (1964).
49. (a) D. L. Huestis, et. al., Report AD-A009284, (NTIS, 31 Jan., 1975);
(b) C. D. Cooper, G. C. Cobb, and E. L. Tolnas, *J. Molec. Spectrosc.* 7, 223 (1961).
50. A. Elizary, D. L. Barton, and A. Baltonoff, *Proc. IEEE*, 62(8), 1119 (1974).
51. (a) J. A. Browder, R. L. Miller, W. A. Thomas, and G. Sanzone, *Internat. J. Mass Spectrom. Ion Phys.*, 37, 99 (1981).
(b) J. A. Browder, R. L. Miller, A. Smith, and G. Sanzone, Manuscript in preparation for submission to *Rev. Sci. Instr.*

52. C. W. Werner, E. V. George, P. W. Hoff, and C. K. Rhodes, *Appl. Phys. Letters* 25, 235 (1974).

53. (a) L. A. Schlie, B. D. Guenthe, and R. D. Rathge, *Appl. Phys. Lett.* 28, 393 (1976);
(b) R. E. Drullinger, M. M. Hessel, and E. W. Smith, *J. Chem. Phys.* 66, 5656 (1977);
(c) H. Komine and R. L. Byer, *J. Chem. Phys.*
(d) Math. Sciences Northwest, Inc. Report 77-1077-1 (7 Oct., 1977);
(e) J. R. Woodworth, *J. Chem. Phys.* 66, 754 (1977).

54. (a) M. S. Kim, R. E. Smalley, L. Wharton, and D. H. Levy, *J. Chem. Phys.* 65, 1216 (1976);
(b) R. E. Smalley, D. H. Levy, and L. Wharton, *J. Chem. Phys.* 64, 3266 (1976).

VIII: PERSONNEL

1. Principal Investigator

(a) Dr. George Sanzone (Chemistry Dept.)

Was medically disabled for past two years; now mended and working.

2. Associate Investigators: Experiment

(a) Dr. James A. Jacobs (Physics Dept.)

Died in 1978.

(b) Dr. John C. Hassler (Chemical Engineering)

Failed to obtain tenure; presently at Univ. of Maine.

3. Associate Investigators: Theory

(a) Dr. John C. Schug (Chemistry Dept.)

(b) Dr. Clayton D. Williams (Physics Dept.)

Took position as associate department head.

4. Post-Doctoral Associates

(a) Dr. Thomas T.-S. Huang

calibration measurements of cluster beam;

now Chairman, Dept. of Chemistry, East Tenn. State Univ.

(b) Dr. Dana Brewer

calibration of laser system;

now at NASA-Langley Research Center.

5. Graduate Students

(a) Raymond W. Mattozzi

Assembly and test of cluster beam;

failed to complete degree.

(b) Eileen O'Brien

Calculations of Hg_2 potential energy curves;

failed to complete degree.

(c) Edward Rickman

Work on the excitation electron gun led him into study of
charge-exchange kinetics.

6. Undergraduate Students

- (a) Ellen J. Bonham (Chemistry)
- (b) Sally A. Reed (Chemistry)
- (c) Eric Raitch (Mechanical Engrg.)
- (d) John Scott Davis (Chem. Engrg.)

7. Technicians

- (a) William P. Kahler
Developed quadrupole electronics.
- (b) Chris Arrians
Operation of molecular beam;
left project to have baby (a productivity unrelated to this
research).

END

DATE FILMED

10/08/81